RSC Sustainability

ROYAL SOCIETY OF CHEMISTRY

CRITICAL REVIEW

View Article Online
View Journal | View Issue

Cite this: *RSC Sustainability*, 2026, **4**, 1160

A review of aqueous-based binders used for cathode fabrication in lithium-ion batteries

Samuel O. Ajayi,*[a] Tarekegn H. Dolla,[a] Peter R. Makgwane,[a] Xinying Liu,[a] Moses M. Solomon,[b] Cyril O. Ehi-Eromosele[c] and Mkhulu K. Mathe*[a]

Lithium-ion batteries have emerged as the leading energy storage technology for electric vehicles and devices due to their high energy density and rechargeability. Although binders constitute less than 5 wt% of the electrode composition and contribute minimally to the overall LIB cost (<2%), they have a significant impact on battery performance, particularly on cycling stability. Poly(vinylidene fluoride) remains the most widely used binder in LIB cathodes, but it is typically processed using *N*-methyl-2-pyrrolidone, a flammable and harmful solvent. Consequently, these limitations have stimulated the research and development of environmentally sustainable and economically viable alternatives, referred to as aqueous binders. While aqueous binders have been extensively investigated for anode fabrication, their use in cathode materials is more challenging due to the higher reactivity of the cathode materials with water than that of anodes. This review presents an overview of commonly employed aqueous binders for LIB cathodes, with particular focus on carboxymethyl cellulose, poly(acrylic acid), and chitosan. Their electrochemical performances are critically evaluated in comparison with the conventional PVDF binder. The aqueous binders enhance cathode performance through improved dispersion, adhesion, and interfacial stability. They also exhibit reduced charge-transfer resistance and better Li^+ transport due to strong ionic interactions and compact electrode formation. In addition, the challenges inherent in aqueous binder systems such as crack formation, lithium leaching and Al current collectors are examined. pH control using weak acids such as phosphoric acid and carbon-coated aluminum collectors mitigates Al corrosion and crack formation during aqueous processing. The industrial perspective of aqueous binder implementation in LIB cathode fabrication is also discussed.

Received 7th November 2025
Accepted 25th January 2026

DOI: 10.1039/d5su00849b

rsc.li/rscsus

Sustainability spotlight

The conventional cathode binder, poly(vinylidene fluoride), requires the use of the toxic *N*-methyl-2-pyrrolidone, which raises safety and environmental concerns. Consequently, these limitations have stimulated the research and development of environmentally sustainable and economically viable alternatives, referred to as aqueous binders. While aqueous binders are widely adopted in anodes, cathode applications remain challenging due to water reactivity. This review highlights aqueous binders as sustainable and promising alternatives to poly(vinylidene fluoride) in lithium-ion battery cathodes. These binders improve adhesion, dispersion, and Li^+ transport, while pH control and carbon-coated Al collectors mitigate corrosion issues. Industrial perspectives on aqueous binder integration for greener cathode manufacturing are critically discussed.

1 Introduction

Global warming and environmental pollution pose critical challenges for contemporary society. The development and implementation of clean energy systems are vital for diminishing reliance on fossil fuels and alleviating the associated ecological impacts. Transitioning to renewable energy sources is imperative for reducing greenhouse gas emissions and fostering sustainable environmental practices.[1] Energy storage devices, such as secondary batteries, fuel cells, and supercapacitors, have garnered a lot of interest due to their high efficiency in converting chemical energy into electrical energy. Among these, LIBs are widely utilized in electric vehicles and devices owing to their high energy density and rechargeability.[1,2] However, in comparison to conventional combustion engines, their energy density and cycling performance need to be improved for electric vehicles.[3] To address these limitations, research efforts are increasingly focused on the synthesis of novel electrode materials with enhanced capacity and stability.[1,4]

[a]*Institute for Catalysis and Energy Solutions (ICES), College of Science Engineering and Technology, University of South Africa, Johannesburg, Florida 1709, South Africa. E-mail: ajayiso@unisa.ac.za*

[b]*Department of Chemical and Environmental Engineering, University of Nottingham Ningbo China, Ningbo 315104, China*

[c]*Department of Chemistry, Covenant University, P.M.B. 1023, Ota, Nigeria*

Studies have shown that the materials, structure, and method of fabrication of an LIB have a significant impact on its electrochemical characteristics.[1] The conductive additive, binder, and active material are combined on the current collector to form the electrode composite.[1]

The binder helps maintain adhesion by attaching the active material and the conductive additive to the current collector. The conductive additive improves electron transport between the active material and the current collector. Additionally, the active material determines the overall energy density of the electrode.[1] The binder is essential to the operation of the battery, particularly for maintaining cycling performance, even though it is used in very small quantities (less than 5 weight%) and contributes less than 2% to the total cost of the LIBs. Without the use of a binder, the active components on a standard electrode will progressively lose their electrical and physical contact with the foil or current collector.[1,5]

Thus, a perfect binder for LIBs should possess a combination of critical properties, including mechanical flexibility, high thermal stability (electrochemical and chemical), nominal swelling, electrolyte insolubility, adequate adhesive strength, efficient electronic and ionic conductivity, and the capacity to form a homogeneous slurry for the uniform coating of active materials on foil or current collectors. Additionally, cost-effectiveness and environmental sustainability are essential for practical and commercial viability.[6]

The most widely used binder for preparing LIB electrodes is polyvinylidene fluoride (PVDF), which is typically processed using the toxic and flammable solvent *N*-Methyl-2-pyrrolidone (NMP). Beyond its high cost, PVDF poses safety concerns; under elevated temperatures, it undergoes exothermic reactions with lithium metal or lithiated graphite, generating lithium fluoride (LiF) and unsaturated fluorinated compounds, thereby contributing to thermal runaway in LIBs.[6]

PVDF binder can undergo decomposition under certain conditions, leading to the release of hydrogen fluoride (HF), which reacts exothermically with lithium salts, generating heat within the cell. Additionally, although PVDF melts at about 177 °C, it can soften and lose adhesion under thermal abuse or elevated operating temperatures. This compromises the structural integrity of the electrode and speeds up the degradation of the LIB's capacity.[6] Also, the high boiling point of NMP significantly increases the energy demand for solvent removal during electrode preparation, thereby hindering the cost-effectiveness and environmental sustainability of LIB production. Consequently, the development and implementation of green alternatives to PVDF are essential for advancing more economical and eco-friendly electrode manufacturing processes.[5–7]

It is noteworthy that aqueous binders have been more extensively applied and have attracted greater attention in the fabrication of LIB anodes than cathodes, primarily due to the higher reactivity of cathode materials with water. However, significant recent efforts have focused on extending the application of aqueous binders to cathode materials to enable more cost-effective and environmentally sustainable electrode processing in LIBs. Also, studies have highlighted the role of aqueous binders in LIB cathode fabrication, emphasizing their advantages in improving electrode cohesion, enhancing adhesion to current collectors, and acting as rheological modifiers to stabilize slurry dispersion and regulate viscosity during processing.[5–7]

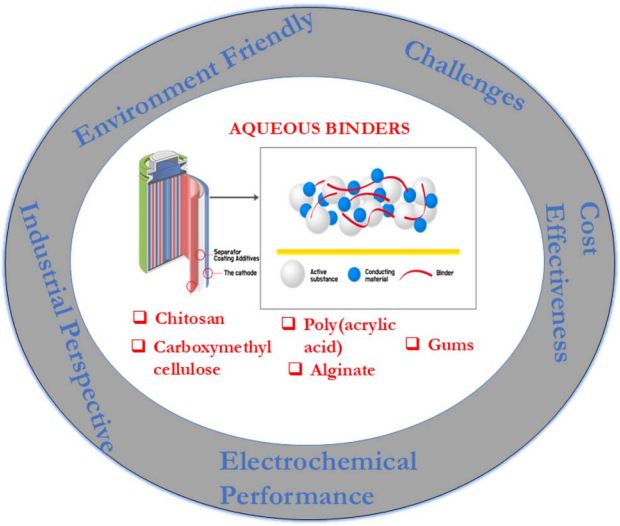

Fig. 1 Schematic of the potential of aqueous binders.

This review presents a concise overview of various cathode materials for LIBs, with an emphasis on the different types and applications of aqueous binders (Fig. 1). Particular emphasis is placed on the use of CMC, PAA, and chitosan (CTS) as alternative binders. The electrochemical performance of aqueous binders is critically evaluated and compared with that of the conventional PVDF binder. In addition, the discussion highlights their sustainability considerations and elucidates how the functional groups of these binders influence the electrochemical performance of cathode materials. Furthermore, the challenges associated with aqueous binder systems are discussed. This work also provides the first comprehensive discussion on the industrial perspective of aqueous binder applications in LIB cathode fabrication.

2 Different types of cathode materials used in LIBs

The advancement of LIBs critically depends on the synthesis of novel cathode materials and a comprehensive understanding of the relationships among their structure, composition, and electrochemical performance, particularly in terms of energy density and cost effectiveness.[6] The commercial LIB cathode materials are generally classified into three main categories: layered oxides, spinel structures, and olivine compounds.[6] These materials are predominantly based on transition metal oxides or phosphates.[6,8–11] The layered transition metal oxides represent the most promising category of cathode materials for LIBs. Examples include $LiCoO_2$, $LiNiO_2$, and $LiMnO_2$, all of which have been extensively studied. However, the key limitation of these materials is their capacity fade over long cycling. Thus, the synthesis of mixed transition metal (TM) oxides, such

as $LiNi_{1-a-b}Co_aMn_bO_2$ and $LiNi_{1-a-b}Co_aAl_bO_2$, was proposed to enhance the structural stability and electrochemical performance of layered oxides.[6,12–15] Spinel oxides ($LiMn_2O_4$) and olivine phosphates ($LiFePO_4$) are two alternative classes of cathode materials to layered oxides.[6,16–18] However, these materials possess relatively low energy densities, which constrain their practical applications in commercial LIBs.

Researchers have worked hard to investigate new high-capacity (greater than 200 mAh g^{-1}) and high-voltage (>4.0 V *vs.* Li^+/Li) cathodes to significantly enhance the LIBs energy density. Metal-rich layered oxides have emerged as highly promising candidates for next-generation LIBs, owing to their exceptional energy storage capabilities.[6,19,20] Notable examples include $LiNi_{0.8}Co_{0.1}Mn_{0.1}O_2$ and $LiNi_{0.8}Co_{0.15}Al_{0.05}O_2$, which exhibit high gravimetric and volumetric capacities around 200 mAh g^{-1} and 932 mAh cm^{-3} for $LiNi_{0.8}Co_{0.1}Mn_{0.1}O_2$, and 220 mAh g^{-1} and 980 mAh cm^{-3} for $LiNi_{0.8}Co_{0.15}Al_{0.05}O_2$.[6,21] Additionally, $LiNi_{0.5}Mn_{1.5}O_4$ operates at 4.7 V *versus* Li^+/Li and offers a gravimetric capacity of 147 mAh g^{-1} and a volumetric capacity of 626 mAh cm^{-3}.[6,22] Recently, Li-rich layered oxides, $[(xLi_2MnO_3 \cdot (1-x)LiTMO_2$, TM = Mn, Co, Ni)], were reported as promising cathodes with high practical capacities of about 280 mAh g-1 at 2.0–4.8 V.[23–30]

3 Overview of aqueous binders for LIBS

The word "green" is frequently used to describe environmentally friendly materials and methods, but the context in which it is used can greatly alter its meaning.[31] Green alternatives for polymeric binders could be classified based on natural availability, chemical composition, and processability as presented in Fig. 2. Binders that are soluble/dissolve in environmentally benign solvents, like ethanol or water, can be categorized as green substitutes based on their processability. Poly(-tetrafluoroethylene) (PTFE) is a very hydrophobic polymer that is characterized by strong C–C and C–F bonds. It offers high chemical and mechanical stability properties and is thus widely utilized in the fabrication of highly durable coatings and membranes.[31,32] The ability of PTFE to form a dispersion in water and be stabilized by wetting agents enables its use in electrode processing. However, wetting agents like carboxylic acids containing fluorine are harmful to the environment and/or to life. Therefore, this binder is not particularly environmentally friendly based solely on the possibility of aqueous processing.[31]

Fluorinated acrylate polymer latex is another water binder commercialized by JSR Corporation (Japan).[33,34] It offers low interfacial resistance, long cycle life and higher bonding to the foil/current collector.[31] It is noteworthy that fluoropolymers are more difficult to get rid of at the end of the battery's life, in spite of their water processability that lessens the environmental impact of electrode fabrication. Notably, aside from a few expensive and hazardous solvents such as *N*,*N*-dimethylformamide (DMF), *N*,*N*-dimethylacetamide (DMA), NMP, and dimethyl sulfoxide (DMS), fluoropolymers are generally insoluble in most common solvents. It is difficult to isolate the fluorinated binding agents from the electrode active materials. Thus, it requires thermal treatment for removal, leading to the release of highly toxic and ozone-depleting fluorinated decomposition products. Consequently, there is a need for fluorine free binders for electrode coating for LIBs.[31]

Various polymers, such as polyacrylates (PAA), polystyrene (PS) and polyethylene (PE), have been projected as alternative

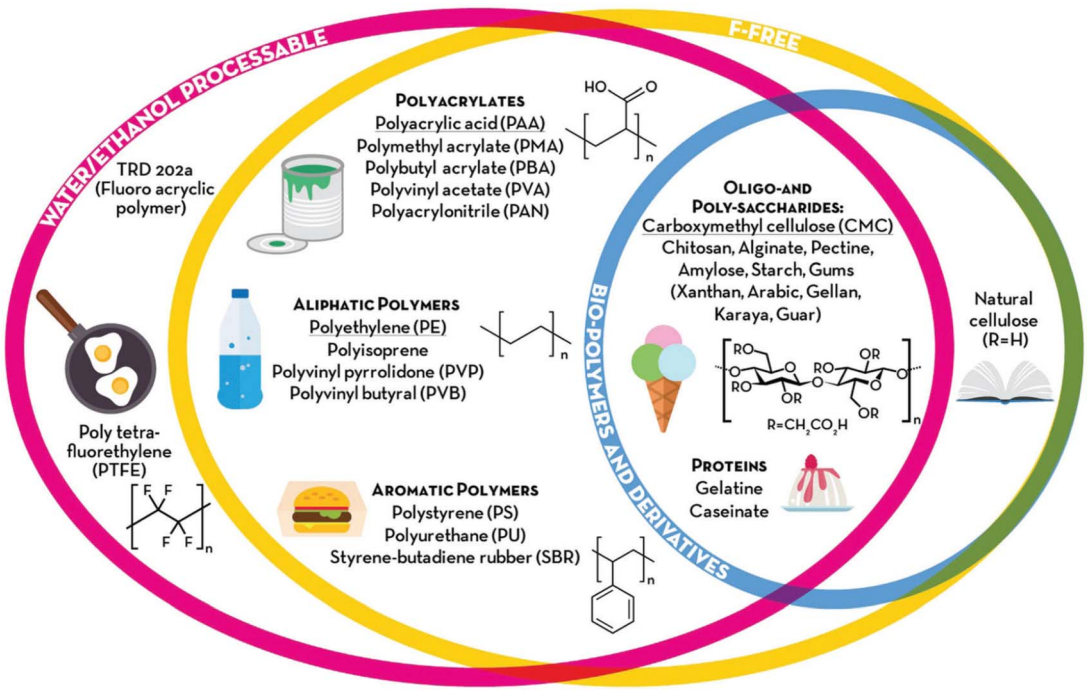

Fig. 2 Classification of the aqueous binders. Reproduced with permission from ref. 31. Copyright 2018, The Royal Society of Chemistry.

Fig. 3 Advantages of the aqueous binders.

binders for LIBs electrode processing. The soft and rubbery properties of these materials typically exhibit low glass transition temperatures (T_g), facilitating processing and enhancing the mechanical stability of electrodes, thereby potentially improving cycling performance. However, the electrode fabrication using these polymers depends on non-renewable materials. Thus, a more sustainable alternative is the use of biopolymers and their derivatives.[31]

Polysaccharides, a class of naturally occurring polymers, can be extracted from various non-edible sources. While they are generally composed of glucose monomers, their distinct physicochemical properties arise from variations in glycosidic linkages and substitutions on the pyranose ring, as exemplified by cellulose, alginate, and starch.[31]

Carboxymethyl cellulose (CMC), a bio-derived polymer, in combination with styrene-butadiene rubber (SBR), is among the most widely employed binder systems in the advanced fabrication of LIB electrodes.[31] While its main role in electrode processing is as a rheology modifier that stabilizes the slurry and adjusts its viscosity,[31] it also contributes to electrode cohesion and binding. Its water solubility is achieved by partially substituting hydroxyl groups with carboxymethyl (–CH_2COOH) functional groups.[31]

Generally, aqueous-based binders offer advantages such as greater tolerance to air and humidity during processing, cost-effectiveness, and environmental friendliness (Fig. 3).[35] Notably, their sustainability is particularly highlighted by the avoidance of NMP solvents. As illustrated in Fig. 4, aqueous-based binders offer several benefits over their non-aqueous counterparts (PVDF binder) in electrode fabrication. These include rapid solvent evaporation, lower binder content (~5%), which contributes to higher cell energy density, and reduced swelling in carbonate-based electrolytes. Furthermore, aqueous binders are more cost-effective due to their lower material cost and simplified processing requirements.[35,36]

4 Common aqueous binders used in the preparation of LIB cathode material

4.1 Carboxymethyl cellulose

CMC is a linear polymeric cellulose derivative made up of β-linked glucopyranose skeleton units with different degrees of carboxymethyl group substitution.[6] In cathode fabrication,

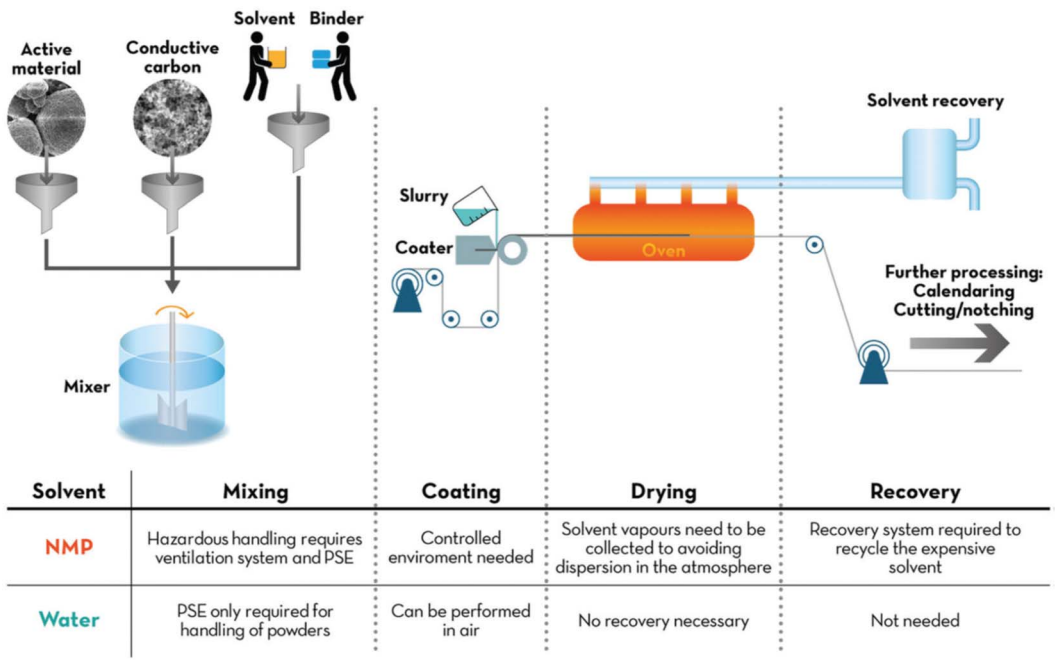

Solvent	Mixing	Coating	Drying	Recovery
NMP	Hazardous handling requires ventilation system and PSE	Controlled enviroment needed	Solvent vapours need to be collected to avoiding dispersion in the atmosphere	Recovery system required to recycle the expensive solvent
Water	PSE only required for handling of powders	Can be performed in air	No recovery necessary	Not needed

Fig. 4 Illustration of the battery manufacturing process and the advantages of employing water rather than NMP. Reproduced with permission from ref. 31. Copyright 2018, The Royal Society of Chemistry.

CMC functions as a thickening agent and is mostly utilized in mixtures with SBR to lessen active material sedimentation.[37] CMC has been widely used in aqueous processed cathode fabrication. Guerfi *et al.*[38] combined CMC and water-soluble elastomer binder in a 1 : 1 ratio for the $LiFePO_4$ cathode. The elastomer made contact with a small portion of the $LiFePO_4$ particle surface, resulting in excellent mechanical elasticity and enhanced adhesion with the aluminum foil. The resulting CMC-based cathode gave a superior first discharge capacity of 157 mAh g^{-1}, in comparison to 148 mAh g^{-1} for a conventional PVDF-based $LiFePO_4$. Also, the resulting CMC-based $LiFePO_4$ gave a superior electrode density of 1.7 g cm^{-3}, compared to 1.5 g cm^{-3} for a conventional PVDF-based cathode, thereby enhancing the volumetric energy density of the CMC-based cathode.[38] Compared to the PVDF-based cathode, the CMC-based cathode exhibits greater compactness, enabling a reduction in post-preparation treatment, which lowers processing time and costs. Lux *et al.* enhanced the rate capability and capacity retention of the $LiFePO_4$ cathode using CMC binder compared to the conventional PVDF-based binder.[39]

Studies have shown that CMC has minimal influence on electron transport within the electrode due to its electrochemical inertness.[6] Thus, incorporating electronically conductive polymers into CMC enables the formation of a conductive binder medium, thereby improving the electrode's electrochemical properties.[6,40] Yang *et al.*[40] reported the effect of a humics/CMC (HAC) binder on the $LiFePO_4$ cathode. Humic substances are characterized by aromatic rings and polar functional groups that create a conductive network *via* π–π conjugation, effectively linking cathode components and aiding electron transport. The electrochemical results show that the humics/CMC binder greatly enhanced the $LiFePO_4$ cathode performance compared to the PVDF and CMC binders. The humics/CMC binder-based $LiFePO_4$ cathode delivered the best discharge capacity (152.3 mAh g^{-1}), capacity retention (99.2%) after 100 cycles, and the best rate capability compared to CMC binder- and PVDF binder-based $LiFePO_4$ cathodes (Fig. 5a and b).[40]

Kim *et al.*[41] reported a benign and environmentally friendly LIB cell incorporating Na-CMC binder in a cell containing a $LiFePO_4$ cathode, $Li_4Ti_5O_{12}$ anode and *N*-butyl-*N*-methyl-pyrrolidinium bis(fluorosulfonyl)imide electrolyte. At 25 °C, the cell gave a specific capacity of 140 mAh g^{-1} and maintained a stable performance over 150 cycles. Qiu *et al.*[42] employed CMC-Li as a binder for $LiFePO_4$, in place of the conventional PVDF binder. Their findings showed that the CMC-Li-based $LiFePO_4$ displayed a reversible capacity of 175 mAh g^{-1} after 200 cycles, with minimal capacity fade and superior cycling stability compared to the PDVF-based counterpart.[42] The enhanced electrochemical performance was attributed to the ability of CMC-Li to facilitate an efficient conductive network within the $LiFePO_4$ structure.[7,42] Eliseeva *et al.*[43] investigated the influence of a composite conducting binder, PEDOT:PSS/CMC, on C–$LiFePO_4$ cathodes. In this composite, CMC acted as a supplementary binder and thickener with strong ionic conductivity, while PEDOT:PSS served as a conductive binder additive. The resulting cathode delivered a discharge capacity of 126 mAh g^{-1} at 5 C, along with excellent cycling stability and rate capability. Thus, the conductive composite binder enhanced the electrochemical performance of the C–$LiFePO_4$ cathode.[7,43]

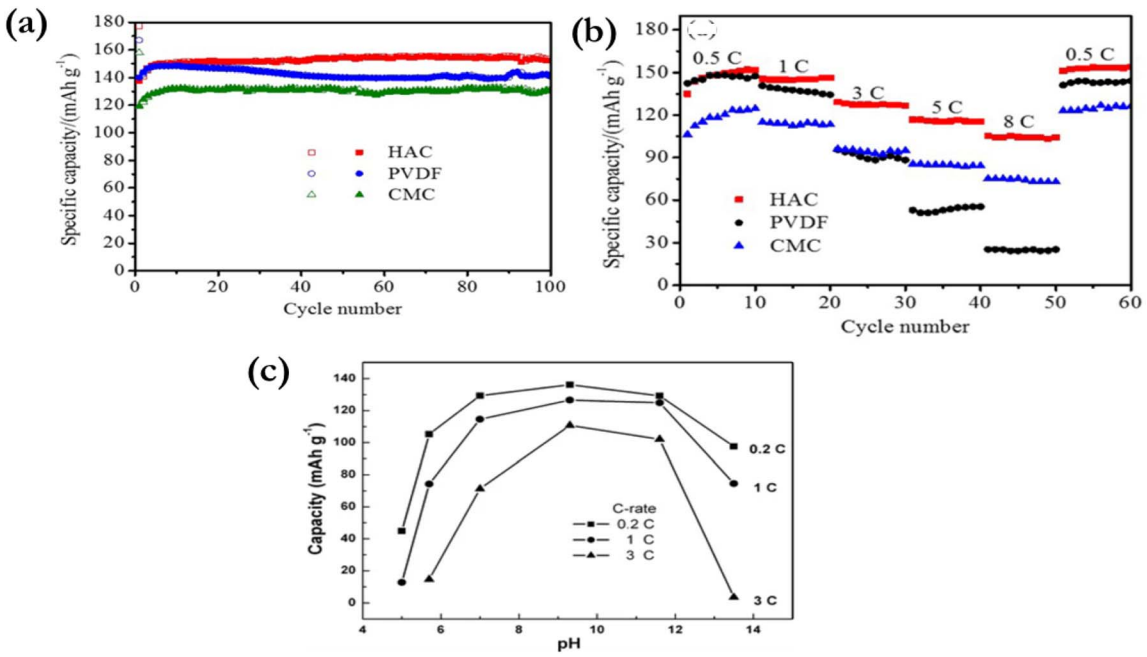

Fig. 5 (a) Cycling performance. (b) Rate capability of $LiFePO_4$ with the humics/CMC, PDVF and CMC binders. Reproduced with permission from ref. 40. Copyright 2019, Elsevier. (c) Effects of pH at different discharge rates for the $LiCoO_2$/Li half-cells. Reproduced with permission from ref. 46. Copyright 2017, Springer.

Zheng *et al.*[44] employed a CMC–NH_4 binder for the fabrication of $LiFePO_4$ cathodes and reported superior electrochemical performance compared to conventional PVDF-based systems. The CMC–NH_4-based cathode demonstrated a capacity retention of 86.6% after 400 cycles at 1 C, which is significantly higher than the 60.7% observed for the PVDF-based counterpart. The enhanced performance was credited to the existence of amino groups, which improved interfacial bonding with the cathode material and increased electrolyte affinity. Additionally, these functional groups provided more adsorption sites for Li^+ ions, thereby enhancing ionic conductivity and overall electrochemical performance.[44]

Li *et al.*[45] investigated how the SBR and Na-CMC blending ratio affected the dispersion behaviour and electrochemical performance of the $LiCoO_2$ cathode. Their results revealed that the lower the SBR fraction, the better the slurry dispersion, which led to less uniform binder spreading in the dried electrode, subsequently resulting in higher surface resistance and lower electrode adhesion strength. It is worth noting that the pH of an aqueous slurry has a significant impact on its dispersion properties and cell performance.[45]

Li *et al.*[46] investigated the relationships between dispersion behavior and the pH of $LiCoO_2$-based aqueous slurries containing Na-CMC (0.64 wt%) and SBR (0.96 wt%) binders. Their findings showed that the aqueous slurry formed a homogeneous electrode at the initial equilibrium pH of 11.6. Nevertheless, at elevated pH levels, the slurries react extensively with the aluminum foil/current collector, causing damage to the microstructure of the $LiCoO_2$ cathode and impairing cell performance. Optimal adhesion strength and electrochemical performance were observed at pH 9.3 for $LiCoO_2$ (Fig. 5c), and it was attributed to enhanced dispersion uniformity and improved electron transport at the electrode–current collector interface.[46]

Chen *et al.*[47] developed a Na-CMC binder for high-voltage $LiCoO_2$ (4.6 V) cathodes using a thermal pulse sintering method to modify the molecular structure of CMC at various temperatures. This treatment induces an open-ring reaction, leading to the formation of ether linkages through the electrochemical decomposition of active carboxyl groups, thereby creating additional Li^+ transport pathways on the cathode surface. Furthermore, the process promotes uniform binder coating, forming a robust protective layer that mitigates interfacial side reactions. The Na-CMC-based $LiCoO_2$ cathode demonstrated excellent cycling stability, achieving 93% capacity retention after 200 cycles.[47]

Xu *et al.*[48] compared the electrochemical performances of synthesized NMC111 cathodes using Na-CMC, alginate, and PVDF binders. While the CMC-based cathode exhibited the lowest first discharge capacity, it demonstrated superior cycling stability and rate capability compared to PVDF and alginate-based cathodes (Fig. 6a–c). The CMC, PVDF and alginate-based cathodes delivered discharge capacities of 107.9, 8, and 76.8 mAh g^{-1}, respectively, after 100 cycles at 5 C. The superior performance of the CMC-based cathode is credited to lower charge transfer resistance and lesser activation energy, which eases Li^+ ion transport during cycling.[48]

Doberdò *et al.*[49] prepared NMC111 cathodes using a Na-CMC binder in aqueous media, employing carbon-coated (C) aluminum foil as the current collector to mitigate corrosion of the aluminum substrate during electrode processing. The Na-CMC-based electrode with a 5 μm carbon coating on aluminum foil delivered a 126 mAh g^{-1} discharge capacity after 50 cycles at 1 C. While its initial discharge capacity was slightly lower than that of the PVDF-based counterpart, it demonstrated superior capacity retention with minimal fading over cycling.[49]

Loeffler *et al.*[50] investigated the effects of various calendering forces on CMC-based NMC111. They discovered that calendering has a significant influence on the morphology of the cathode, and so adhesion has a positive effect on cycle performance.[50]

Kukay *et al.*[51] studied the effects of phosphoric acid (PA) addition on NMC 811 cathodes treated with CMC-fluorinated acrylic hybrid latex binders in a 1 : 4 ratio. The use of phosphoric acid reduced crack formation and corrosion in the cathode, thus improving its discharge capacity, rate performance and capacity retention. Furthermore, PA modified the rheological properties of the cathode slurry due to the electrode's surface and increased gravitational force.[51]

Demiryürek *et al.*[52] investigated the applicability of CMC/SBR and CMC/poly(ethylene oxide) (PEO) mixed binders in NMC 532 materials. They utilized a multilayer coating approach to achieve high active material loading while maintaining crack-free electrodes. Both mixed binder-based cathodes exhibited electrochemical properties similar to those of PVDF-based cathodes. Furthermore, they used this approach in pouch cells through a roll-to-roll pilot-scale production line, highlighting the commercial viability of the approach. After 1000 cycles, the CMC/PEO-based cathode and graphite anode retained 89% of their capacity at a 1 C rate.[52]

Zhu and coworkers[53] reported the electrochemical performance of NMC622 cathodes prepared using Na-CMC and TRD 202A binders. During slurry preparation, acetic acid was introduced to adjust the pH within the range of 7.4 to 12.1. Their findings revealed that the slurry without acetic acid or pH modification corroded the Al current collector, resulting in the creation of huge holes on the cathodes upon drying; however, a slurry with a pH less than 10 yielded a uniform cathode film with no structural defects. Interestingly, cyclic voltammetry revealed that the addition of acetic acid had no impact on the electrochemical behavior of the cathode during cycling processes. An ultrafast laser structuring was applied to fabricate thick electrodes, resulting in a 40 mAh g^{-1} increase in capacity compared to the unstructured counterpart, thus improving electrochemical performance. Furthermore, the rate capability results revealed that slurries with higher pH values exhibited greater discharge capacities at rates over C/5.[53]

Chen and coworkers[54] reported a comparative study on the performance of NMC442 cathodes using Na-CMC and PVDF binders. The Na-CMC-based cathode exhibited a higher electrochemical performance compared to PVDF-based cathodes. The Na-CMC-based cathode showed a homogeneous distribution of active carbon particles and NMC nanobars, which improved particle adherence to the foil and considerably

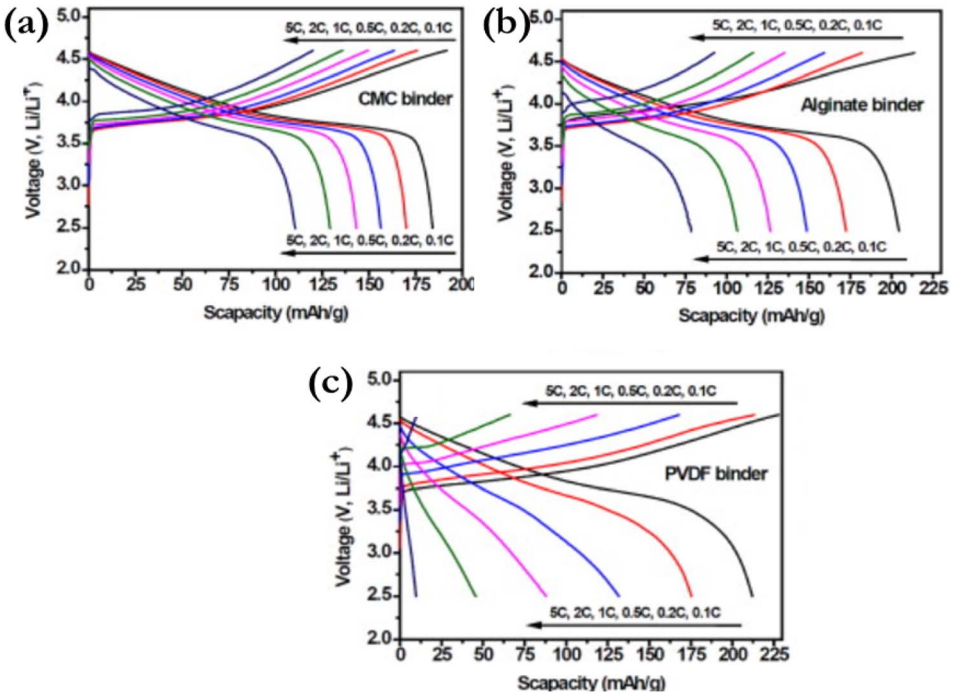

Fig. 6 Initial charge–discharge curves of the NMC111 cathodes at varying rates using various binders (CMC, alginate and PDVF). Reproduced with permission from ref. 48. Copyright 2012, Elsevier B.V.

reduced the creation of cracks in the electrode during frequent lithiation/delithiation operations. The CMC-based cathode exhibited lithium-ion diffusion coefficients approximately twice those of the PVDF-based cathode during both delithiation and lithiation processes, resulting in significantly improved rate capability.

Varshni and Murugan[55] developed a CMC-SBR binder system for $LiNi_{0.7}Mn_{0.25}Al_{0.05}O_2$ (NMA) cathodes, incorporating lithium phytate (LP) as an additive to enhance interfacial stability, structural cohesion, and suppress electrolyte decomposition and the H2-to-H3 phase transition. The resulting CMC-SBR-LP-based NMA cathode demonstrated improved electrochemical performance, achieving 84.2% capacity retention after 200 cycles at 0.5 C and a rate capability of 140.9 mAh g^{-1} at 1 C.[55]

Giorgio and coworkers[56] evaluated the performance of spinel ($LiNi_{0.5}Mn_{1.5}O_4$) cathodes using PVDF and CMC binders. The CMC-based cathode demonstrated superior cycling stability, retaining 83% of its capacity after 400 cycles, compared to 62% for the PVDF-based counterpart. This improved performance is credited to the CMC binder's ability to form a more stable and compact electrode surface, effectively suppressing side reactions at high voltages and thereby enhancing cycle life.[56]

Pace and coworkers[57] reported the electrochemical behaviour of binder systems, such as acrylonitrile multi-copolymer (LA133) + CMC, SBR + CMC, and polytetrafluoroethylene (PTFE) + CMC, in $LiMn_2O_4$ cathode fabrication with an aqueous electrolyte. The results showed that the PTFE + CMC binder system exhibited the best rate performance, attributed to the mechanical robustness of PTFE and the electrolyte swelling capability of CMC.[57]

Dienwiebel and coworkers[58] examined the influence of lithium-based additives (LiOH, $LiNO_3$, and LiTFSI) on the performance of spinel cathodes using CMC-SBR binders. The incorporation of these additives during cathode fabrication effectively suppressed manganese dissolution. Among them, LiTFSI additives showed the most promising results due to their high solubility in the electrolyte, and functioned as conductive salts, enabling electrochemical performance comparable to nonaqueous-based electrodes over 1000 cycles.[58]

Wang and coworkers[59] employed a CMC-based binder for $LiNi_{0.4}Mn_{1.6}O_4$ cathodes, achieving a low self-discharge of 8.8% after three days of rest and a reversible capacity of 139 mAh g^{-1}, approaching the theoretical capacity of 146 mAh g^{-1}.[59]

Li *et al.*[60] substituted PVDF with a CMC-based binder for $Li_{1.2}Mn_{0.56}Ni_{0.16}Co_{0.08}O_2$ cathode fabrication. They reported that the CMC binder enhanced the cycling stability with capacity fading of less than 0.1% per cycle of $Li_{1.2}Mn_{0.56}Ni_{0.16}Co_{0.08}O_2$, compared to 0.2% for the PVDF-based counterpart. The improved performance is attributed to the mitigation of the layered-to-spinel phase transformation.[60]

Zhao and coworkers[61] studied the influence of Na ions in CMC binders on the electrochemical behaviour of $Li_{1.2}Ni_{0.2}Mn_{0.6}O_2$ cathodes. The Na^+ ions from the binder were inserted into the $Li_{1.2}Ni_{0.2}Mn_{0.6}O_2$ during cycling. Interestingly, Na^+ ions occupied Li^+ sites during discharge, leading to an expansion of the interlayer spacing (Fig. 7a). This facilitated Li^+ diffusion and mitigated structural collapse, thereby enhancing cycling stability and rate performance. Furthermore, Zhao *et al.* reported that the use of CMC as a binder enhanced the cyclability and rate capability of $Li_{1.2}Ni_{0.13}Co_{0.13}Mn_{0.54}O_2$ cathodes (Fig. 7b

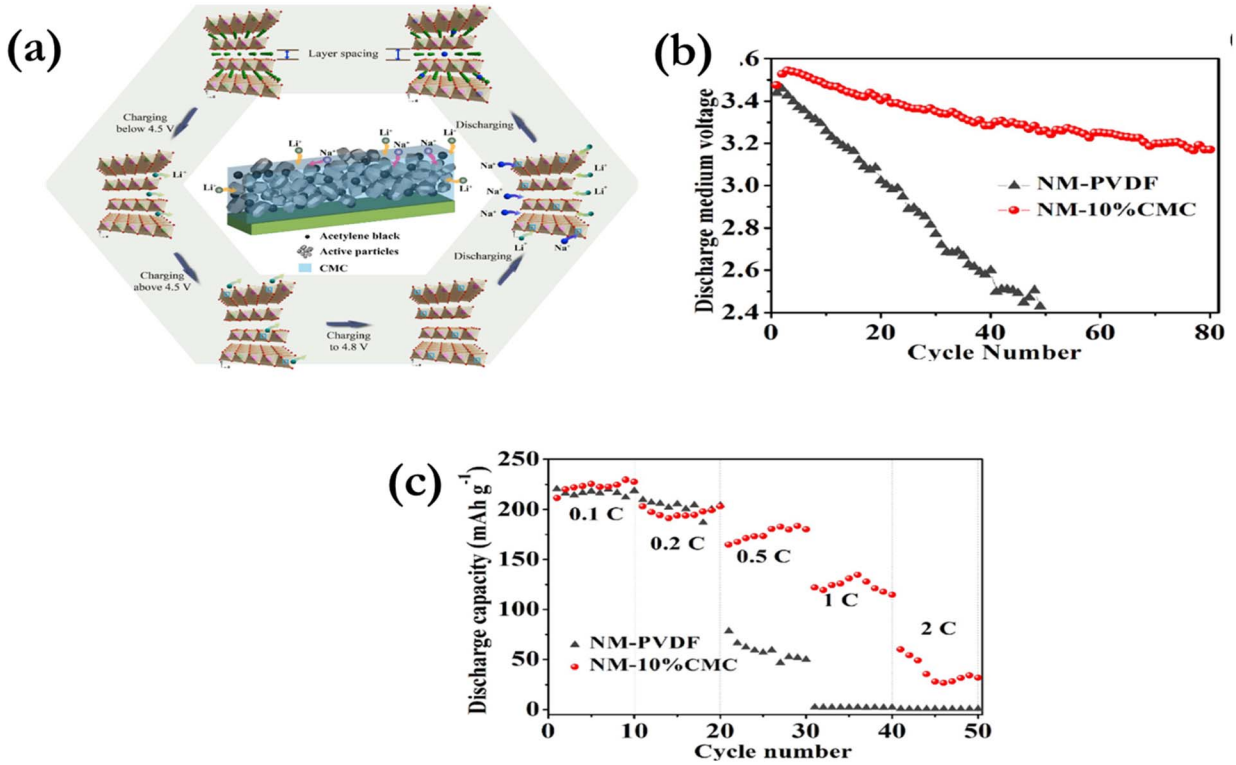

Fig. 7 (a) Schematic showing the mechanism of the first charge–discharge of the CMC-based $Li_{1.2}Ni_{0.2}Mn_{0.6}O_2$, (b) the discharge voltage, (c) and the rate capabilities of the PVDF and CMC-based cathodes. Reproduced with permission from ref. 61. Copyright 2019, Elsevier B.V.

and c). It also improved electrode integrity by promoting durable adhesion to active materials, reducing cracks and minimizing electrode delamination from the current collector.[61]

Zhang *et al.*[62] studied the electrochemical properties of $Li_{1.2}Ni_{0.13}Co_{0.13}Mn_{0.54}O_2$ cathodes fabricated with PVDF, Na-CMC, and polyacrylonitrile (PAN) binders. Both PAN and PVDF-based cathodes exhibited higher initial discharge capacities; however, the CMC-based cathode exhibited higher long-term cyclability. This is attributed to the strong adhesion provided by CMC, which maintains electrical contact and prevents detachment of electrode components from the aluminum foil.[62] X-ray diffraction (XRD) analysis revealed that Na^+ ions from the CMC binder occupy Li^+ vacancies during cycling, inhibiting TM ion migration into lithium layers and thereby mitigating the layered-to-spinel phase transition during cycling. Additionally, Transmission Electron Microscopy (TEM) studies confirmed that the CMC binder significantly reduces the dissolution of TM ions, contributing to the better structural and electrochemical stability of the cathode.[62]

Kazzazi and coworkers[63] studied the influence of three aqueous binders (Na-CMC, sodium alginate (SA), and commercial TRD202A) on the electrochemical performance of $Li_{1.2}Ni_{0.16}Mn_{0.56}Co_{0.08}O_2$ cathodes. Phosphoric acid was introduced during electrode fabrication to suppress aluminum foil corrosion and stabilize the cathode/electrolyte interface. Their findings showed that while the TRD202A binder-based cathode exhibited a slightly higher initial discharge capacity compared to CMC and SA-binder-based cathodes, it experienced more pronounced capacity fading over cycling, indicating inferior long-term stability (Fig. 8a and b). The addition of PA enhanced both the initial capacity and cycling stability across all binder systems.[63]

Ding and coworkers[64] compared Na-CMC and conventional PVDF binders in Li-rich disordered rock-salt oxide cathodes for LIBs. The Na-CMC-based cathode exhibited reduced volume change and improved O^{2-} reversibility during cycling, indicating enhanced structural stability and Li^+ ion kinetics. These factors contributed to superior electrochemical performance relative to the PVDF-based counterpart. Additionally, strong Li^+/Na^+ interactions between the carboxyl groups in CMC and the active material surface improved adhesion, minimizing cathode delamination from the aluminum foil/current collector and promoting the formation of efficient electronic conduction networks.[64]

Su and coworkers[65] developed a high-performance ionic conductive binder by integrating CMC with poly(ethylene oxide) (PEO) *via* hydrogen bonding and incorporating penta-fluorophenylboronic acid (PFPBA) *in situ* to form the CPPFPBA binder, which was stable up to 5.35 V. Applied to Li-rich layered oxide (LRMO) cathodes, the CPPFPBA binder exhibited enhanced cohesion through hydrogen bonding between its hydroxyl and carboxyl groups and the LRMO surface, resulting in more uniform binder distribution compared to CMC alone and CMC:PE (CP) binders, respectively. TEM analysis showed a consistent lattice spacing of 0.24 nm, corresponding to the

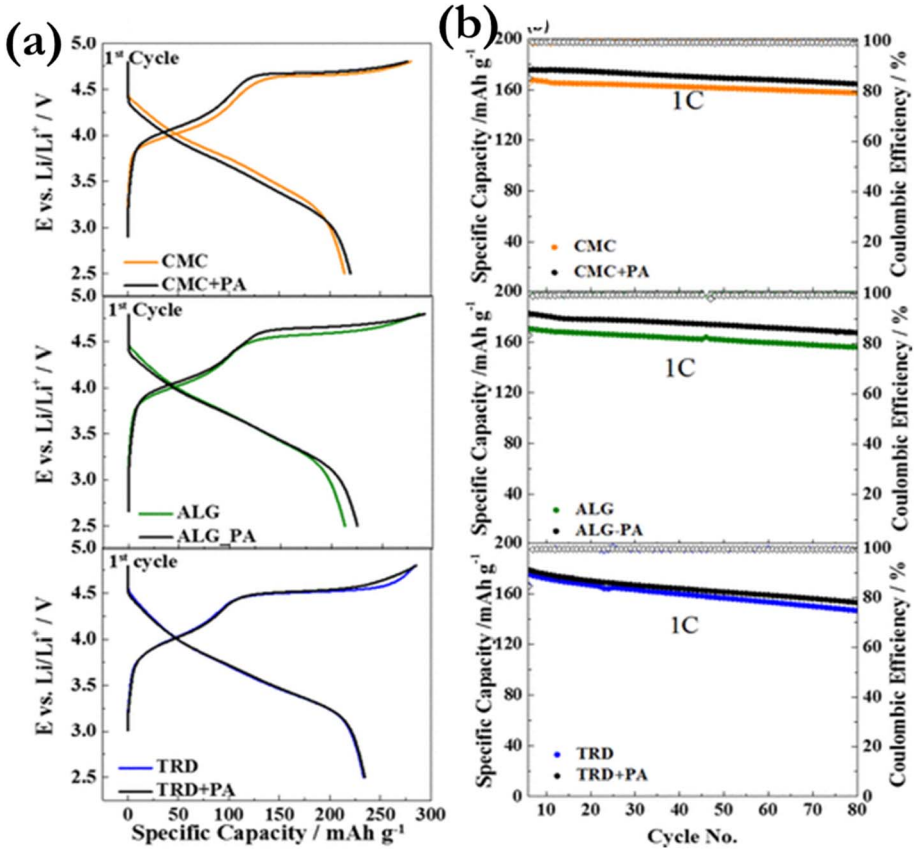

Fig. 8 CMC, ALG, and TRD binders with and without PA (in black and colored): (a) first charge–discharge capacity and (b) cycling performance. Reproduced with permission from ref. 63. Copyright 2018, the American Chemical Society.

(101) plane, in both CMC- and CPPFPBA-based LRMO (Fig. 9a and b). The CPPFPBA-based cathode delivered superior electrochemical performance, including a reversible capacity of 220 mAh g^{-1} after 300 cycles at 200 mA g^{-1}, 102% capacity retention, and enhanced rate capability (Fig. 9c and d). These improvements were attributed to the formation of a uniform fluorine-rich surface layer, which effectively suppressed transition metal dissolution, mitigated side reactions, and reduced voltage decay.[65]

Akhilash *et al.*[66] conducted a comparative study on the $Li_{1.5}Ni_{0.25}Mn_{0.75}O_{2.5}$ cathodes using a CMC–acrylic binder system and a conventional PVDF binder. To optimize slurry pH, a small amount of PA was added during the preparation of the CMC–acrylic binder-based electrode. The initial discharge capacities were 224.94 mAh g^{-1} and 237.7 mAh g^{-1} for the CMC–acrylic and PVDF-based electrodes, respectively. After 100 cycles at a C/10 rate, the CMC–acrylic system retained 219.5 mAh g^{-1} compared to 226.6 mAh g^{-1} for the PVDF counterpart. Notably, the CMC–acrylic binder-based cathode demonstrated superior rate capability at higher current rates (1 C and 2 C), indicating enhanced high-rate performance.[66] Table 1 presents a comparative summary of the electrochemical performance of cathodes utilizing CMC-based aqueous binders relative to their PVDF-based counterparts.

4.2 Poly(acrylic acid) (PAA)

PAA is a polymeric binder consisting of carboxylic groups, which form weak hydrogen bonds with surface hydroxyl groups on cathode materials, thereby creating a conductive ionic layer.[6,35] PAA offers several advantages, including strong adhesion, high mechanical strength, favorable swelling behavior, and uniform particle distribution within the electrode matrix.[67,68] The properties of PAA (electrical) improve with the increase in molecular weight and higher concentrations of Li^+, enhancing its overall electrochemical performance.[69,70] It is worth noting that higher pH values promote better dispersion of electrode particles, but they concurrently compromise the mechanical stability of the PAA binder.[6,35]

The use of PAA as a binder for $LiFePO_4$ cathodes has been extensively investigated.[35] Cai *et al.*[71] demonstrated that the PAA binder-based $LiFePO_4$ cathode exhibited enhanced reversibility compared to those using the PVDF binder counterpart. This was credited to solid electrolyte interphase (SEI) formation with lower resistance and improved Li^+ ion exchange kinetics. The PAA-based $LiFePO_4$ cathode exhibited a higher specific capacity of 134.4 mAh g^{-1}, outperforming the PVDF-based counterpart, which achieved 125.6 mAh g^{-1}. Also, the PAA-based $LiFePO_4$ cathode exhibited superior cycling stability, retaining approximately 98.8% of its initial capacity after 50 cycles, compared to 94.9% for the PVDF counterpart.[71] Zhang *et al.*[72] reported that

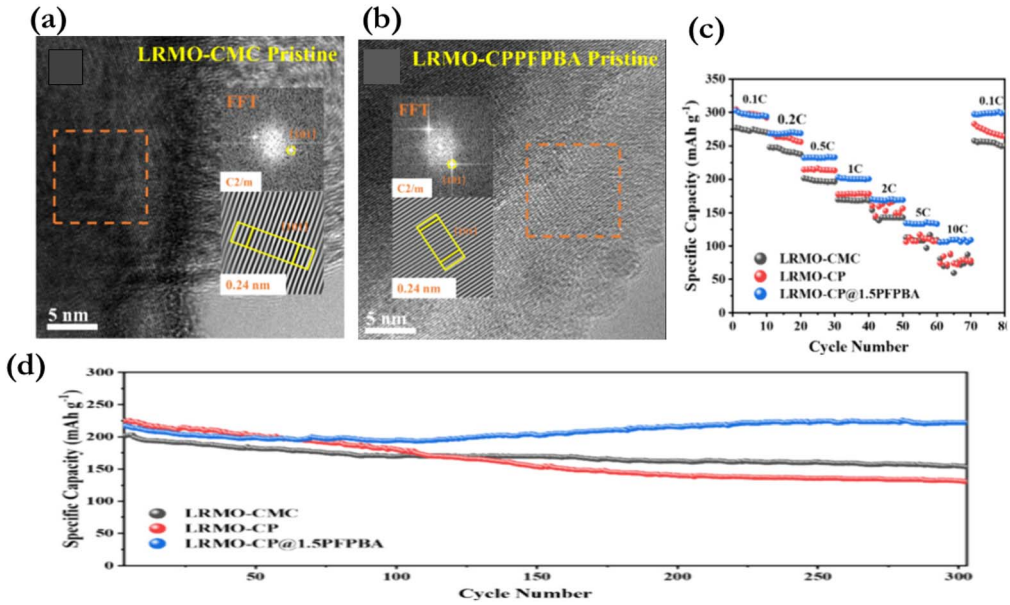

Fig. 9 TEM images of (a) LRMO-CMC and (b) LRMO-CPPFPBA. (c) Rate performance of the electrodes. (d) Cycling performance of the electrodes at 200 mA g^{-1}. Reproduced with permission from ref. 65. Copyright 2025, the American Chemical Society.

the adhesive properties of the PAA binder resulted in the formation of a protective layer around the $LiFePO_4$ cathode, effectively suppressing Fe dissolution and enhancing electrochemical performance at elevated temperatures. Chong *et al.*[73] demonstrated that tuning the mechanical and chemical properties of the binder by blending PAA with SBR enhanced the performance of $LiFePO_4$/graphite cells. The composite binder improved capacity retention to 70% after 850 cycles, while the capacity increased from 147 mAh g^{-1} to 155 mAh g^{-1} due to lowered electrode fracturing associated with the incorporation of SBR.[73] Sun *et al.*[74] developed a $LiFePO_4$ cathode using a PAA binder. The presence of hydroxyl and carboxylic functional groups facilitated the formation of an interconnected network, enhancing binder coverage on the cathode active material surface and improving electrode adhesion. The resulting cathode delivered excellent cycling stability with 100% capacity retention after 300 cycles at 5 C, along with a high-rate performance of 130.1 mAh g^{-1} at 5 C.[74] Wu *et al.* developed a water-soluble polymer binder with a permeating network structure for $LiFePO_4$ cathodes, synthesized *via* high-temperature esterification of lithiated sulfosuccinic acid (LPPS), PVA, and PAA. The resulting gel-like binder reduced interfacial resistance and exhibited strong adhesion to the $LiFePO_4$ cathodes. The $LiFePO_4$/C electrodes demonstrated a specific capacity of 170 mAh g^{-1} and maintained a coulombic efficiency of ~99% after 200 cycles at a 1 C rate.[75]

Vo *et al.*[76] evaluated the electrochemical performance of $LiFePO_4$ cathodes prepared with PVDF and PAA binders at mass ratios of 5%, 10%, and 15%. At 10% binder content, both PAA- and PVDF-based electrodes exhibited mechanical integrity without peeling. However, the PAA-based $LiFePO_4$ cathode achieved a higher discharge capacity (148.9 mAh g^{-1}) and superior coulombic efficiency (97.27%) compared to its PVDF counterpart. Additionally, the 10% PAA-based graphite//$LiFePO_4$ cell demonstrated improved capacity retention and overall performance over 30 cycles.[76]

Shen *et al.*[77] employed a bifunctional PAA binder and coating agent for $LiMn_2O_4$ cathodes, effectively suppressing electrolyte-induced side reactions and Mn dissolution. The PAA-based cathode exhibited 94.1% capacity retention after 1000 cycles at 25 °C and 92.0% after 200 cycles at 60 °C. In 18 650-type cells stored at 60 °C for 25 days in a fully charged state, the voltage drop was limited to 0.1 V with a resistance increase of only 1.25 mΩ, significantly lower than that of the PVDF-based cell. The recovered capacity retention reached 92.2%, outperforming the PVDF counterpart (81.8%).[77]

He *et al.*[78] introduced a terpene resin (TS) emulsion as a tackifier to improve the mechanical integrity of PAALi-based $LiFePO_4$ cathodes. The optimized TS–PAALi (1 : 1) binder exhibited superior flexibility, enhanced adhesion strength (0.170 N cm^{-1}), and improved electrochemical performance, delivering 156.18 mAh g^{-1} with 97.47% capacity retention after 100 cycles and excellent thermal stability at 60 °C, outperforming CMC and PVDF-based electrodes.[78]

PAA shows limited effectiveness in high mass-loading lithium nickel manganese oxide (LNMO) cathodes due to high initial internal resistance arising from contact resistance, non-uniform binder distribution, and inadequate electrolyte wetting. These challenges, particularly agglomeration and pore clogging, can be mitigated through polymer chemistry modifications. Copolymerizing PAA with functional groups enhances adhesion, surface interactions, and electrolyte uptake, thereby improving its suitability for LNMO systems.[79]

Pieczonka *et al.*[80] evaluated LiPAA and PVDF binders for $LiMn_{1.5}Ni_{0.5}O_4$ spinel cathodes. The LiPAA-based cathode exhibited lower impedance, superior cycling stability, and was

Table 1 Comparative electrochemical performances of CMC-based cathodes and their PVDF counterparts[a]

Cathode	Binder	IDC mAh g^{-1}	RC mAh g^{-1}	CR (%)	Ref.
$LiFePO_4$	CMC	157 (C/24)	120 (10 C)	100 (200 cycles at C/1)	38
	PVDF	148 (C/24)	N/A	N/A	38
$LiFePO_4$	CMC	140 (1 C)	130 (5 C)	100 (50 cycles) 75 (1000 cycles at 1 C)	39
	PVDF	152 (1 C)	70 (5 C)	90 (50 cycles at 1 C)	39
$LiFePO_4$	HAC	N/A	105.4 (8 C)	75.9 (100 cycles at 0.5 C)	40
	CMC	N/A	75 (8 C)	67.7 (100 cycles at 0.5 C)	40
	PVDF	N/A	24.1 (8 C)	37.6 (100 cycles at 0.5 C)	40
$LiFePO_4$	Li-CMC	181 (0.1 C)	95 (5 C)	96.69 (200 cycles at 0.1 C)	42
	PVDF	146 (0.1 C)	50 (5 C)	80.6 (200 cycles at 0.1 C)	42
$LiFePO_4$	PEDOT:PSS/CMC	148 (0.2 C)	126 (5 C)	99 (100 cycles at 0.2 C)	43
	PVDF	129 (0.2 C)	101 (5 C)	99 (100 cycles at 0.2 C)	43
$LiFePO_4$	$CMC–NH_4$	N/A	104 (5 C)	86.6 (400 cycles at 1 C)	44
	PVDF	N/A	104 (5 C)	60.7 (400 cycles at 1 C)	44
$LiCoO_2$	SBR and Na-CMC	111.3 (0.2 C)	N/A	N/A	45
$LiCoO_2$	Na-CMC	215 (0.1 C)	152 (4 C)	93% (200 cycles at 1 C)	47
	PVDF	N/A	N/A	90% (200 cycles at 0.2 C)	47
NMC111	Na-CMC	155 (0.5 C)	107.9 (5 C)	90.1% (100 cycles at 0.5 C)	48
	Alginate	150 (0.5 C)	76.8 (5 C)	89.2 (100 cycles at 0.5 C)	48
	PVDF	130 (0.5 C)	8 (5 C)	86.3 (100 cycles at 1 C)	48
NMC111	Na-CMC	126 (1 C)	60 (10 C)	N/A	49
	PVDF	128 (1 C)	68 (10 C)	N/A	49
NMC 532	CMC/PEO	N/A	N/A	89 (1000 cycles at 1 C)	52
	PVDF	N/A	N/A	90 (1000 cycles at 1 C)	52
NMC442	CMC	161.1 (0.1 C)	78.4 (10 C)	99 (100 cycles at 1 C)	54
	PVDF	166.2 (0.1 C)	70.5 (10 C)	80.6 (100 cycles at 1 C)	54
NMA	CMC-SBR/Li-phytate	230.6 (0.1 C)	140.9 (1 C)	97 (200 cycles at 0.2 C)	55
	PVDF	220.69 (0.1 C)	82.95 (1 C)	69 (200 cycles at 0.2 C)	55
$LiNi_{0.5}Mn_{1.5}O_4$	CMC	N/A	45 (10 C)	83 (400 cycles at 1 C)	56
	PVDF	N/A	20 (10 C)	62 (400 cycles at 1 C)	56
$LiNi_{0.4}Mn_{1.6}O_4$	CMC	139 (1 C)	N/A	89 (100 cycles at 1 C)	59
	PVDF	127.9 (1 C)	N/A	95 (100 cycles at 1 C)	59
$Li_{1.2}Mn_{0.56}Ni_{0.16}Co_{0.08}O_2$	CMC	255.4 (0.2 C)	N/A	82.7 (200 cycles at 1 C)	60
	PVDF	266.8 (0.2 C)	N/A	60.4 (200 cycles at 1 C)	60
$Li_{1.2}Ni_{0.2}Mn_{0.6}O_2$	CMC	210.4 (0.1 C)	N/A	119.49 (80 cycles at 0.1 C)	61
	PVDF	219.9 (0.1 C)	N/A	23.33 (80 cycles at 0.1 C)	61
$Li_{1.2}Ni_{0.13}Co_{0.13}Mn_{0.54}O_2$	CMC	247 (20 mAg^{-1})	N/A	83 (500 cycles at 200 mAg^{-1})	62
	PAN	306 (20 mA g^{-1})	N/A	37 (500 cycles at 200 mAg^{-1})	62
	PDVF	297 (20 mA g^{-1})	N/A	40 (500 cycles at 200 mAg^{-1})	62
$Li_{1.2}Ni_{0.16}Mn_{0.56}Co_{0.08}O_2$	CMC PA	214.3 (0.1 C)	N/A	93 (100 cycles at 0.1 C)	63
	ALG	213.2 (0.1 C)	N/A	93 (100 cycles at 0.1 C)	63
	TRD	226.6 (0.1 C)	N/A	83 (100 cycles at 0.1 C)	63
$Li_{1.3}Mn_{0.4}Ti_{0.3}O_{1.7}F_{0.3}$	CMC	186.9 (0.1 C)	80.4 (1 C)	94.5 (30 cycles at 0.1 C)	64
	PVDF	184.4 (0.1 C)	74 (1 C)	80.9 (30 cycles at 0.1 C)	64
$Li_{1.2}Ni_{0.13}Co_{0.13}Mn_{0.54}O_2$	CPPFPBA	297 (0.1 C)	105.72 (10 C)	102(300 cycles at 1 C)	65
$Li_{1.5}Ni_{0.25}Mn_{0.75}O_{2.5}$	CMC–acrylic	224.94 (C/10)	98 (2 C)	97.5 (100 cycles at C/10)	66
	PVDF	237.7 (C/10)	55 (2 C)	95.4 (100 cycles at C/10)	66

[a] IDC-initial discharge capacity; RC-rate capability; CR-capacity retention; N/A-not available; and C-rate and number of cycles are given in parentheses.

resistant to delamination due to stable cathode electrolyte interphase (CEI) formation (Fig. 10a and b). Additionally, LiPAA acted as a lithium-ion reservoir and proton scavenger. The study highlighted LiPAA's improved adhesion, environmental compatibility, and cost-effectiveness over PVDF.[80]

Wang *et al.*[81] developed a multifunctional binder by cross-linking sodium phytate (PN) with PAA for high-voltage NCM811 cathodes. The PAA–PN binder exhibited superior capacity retention of 95.1% at 25 °C and 84.7% at 45 °C after 100 cycles at 4.6 V, outperforming PVDF-based counterparts. This improvement was attributed to the dual protective layers formed by PAA–PN, which suppressed electrolyte decomposition, transition metal dissolution, and intergranular cracking.[81]

Li *et al.*[82] investigated a carbon-modified lithium-rich cathode (C-LRM) using Li-PAA binder (C-LRM-PAA) and compared it with C-LRM using PVDF (C-LRM-PVDF) and a pristine PVDF-based sample (P-LRM-PVDF). The strong hydrogen bonding between Li-PAA's carboxyl groups and the hydroxyl groups of C-LRM ensured tight electrode integration, preventing electrode cracking, while the carbon layer mitigated

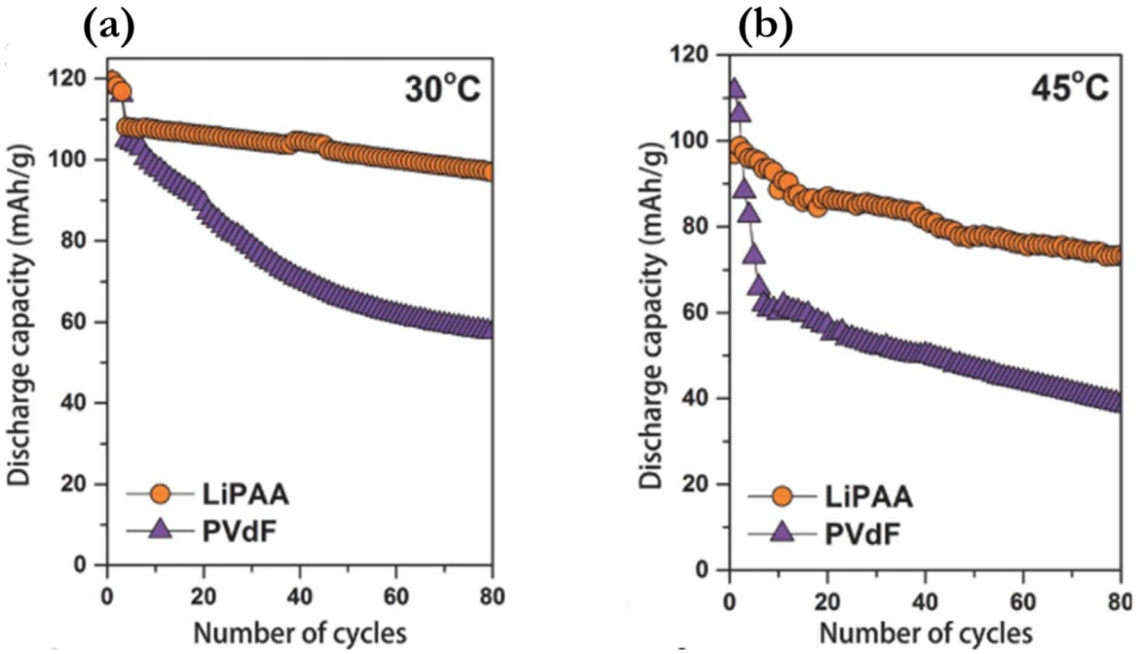

Fig. 10 Capacity retention at 0.5 C-rate at (a) 30 and (b) 45 °C. Reproduced with permission from ref. 80. Copyright 2015, WILEY-VCH.

particle fracture (Fig. 11a). This synergistic effect enhanced Li^+ diffusion, suppressed transition metal dissolution, and reduced charge transfer impedance. After 200 cycles, C-LRM-PAA delivered a discharge capacity of 134.9 mAh g^{-1}, outperforming C-LRM-PVDF (119.8 mAh g^{-1}) and P-LRM-PVDF (71.2 mAh g^{-1}) as presented in Fig. 11b. Additionally, C-LRM-PAA exhibited reduced voltage decay (2.135 mV per cycle *vs.* 2.925 mV per cycle) and superior rate capability (Fig. 11c).[82]

Zhao *et al.*[83] employed a LiPAA binder for LRMO, $Li[Li_{0.2}Co_{0.13}Ni_{0.13}Mn_{0.54}]O_2$) cathodes. The carboxyl groups in LiPAA formed strong hydrogen bonds with oxygen atoms on the active material surface, enhancing structural stability. The LiPAA-based electrode exhibited a reduced voltage drop of 117 mV after 50 cycles, outperforming the PVDF-based counterpart.[83]

Yu *et al.*[84] utilized a LiPAA binder for $Li_{1.15}Ni_{0.17}Co_{0.11}Mn_{0.57}O_2$ cathodes, enhancing cathode particle and current collector adhesion, thus suppressing spinel phase formation during cycling. The LiPAA-based electrode delivered 254.7 mAh g^{-1} with 90.77% capacity retention after 200 cycles at 0.1 C, outperforming the PVDF-based counterpart (223.6 mAh g^{-1}, 76.21% retention).[84]

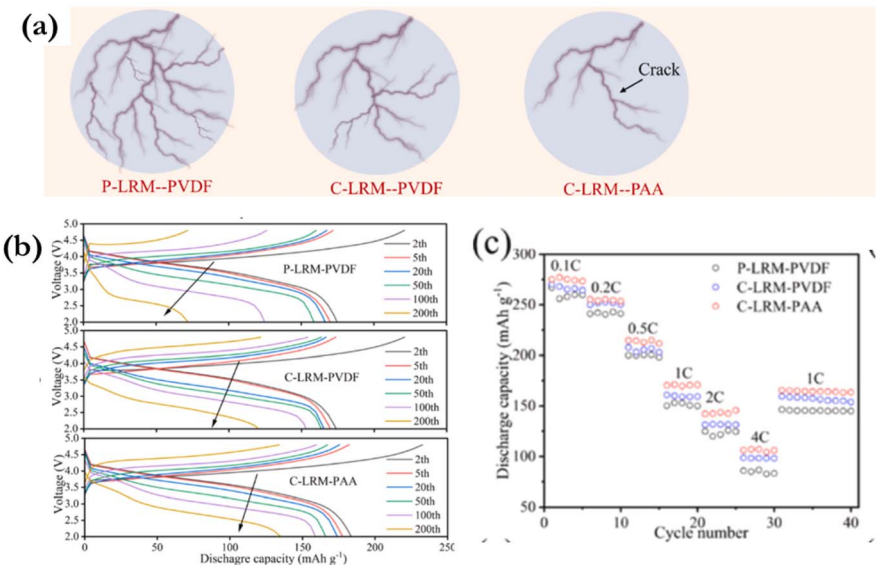

Fig. 11 (a) Schematic of the three-electrode morphology after cycling. (b) Charge–discharge curves of the three electrodes at different cycles and (c) their rate performances. Reproduced with permission from ref. 82. Copyright 2024, Elsevier.

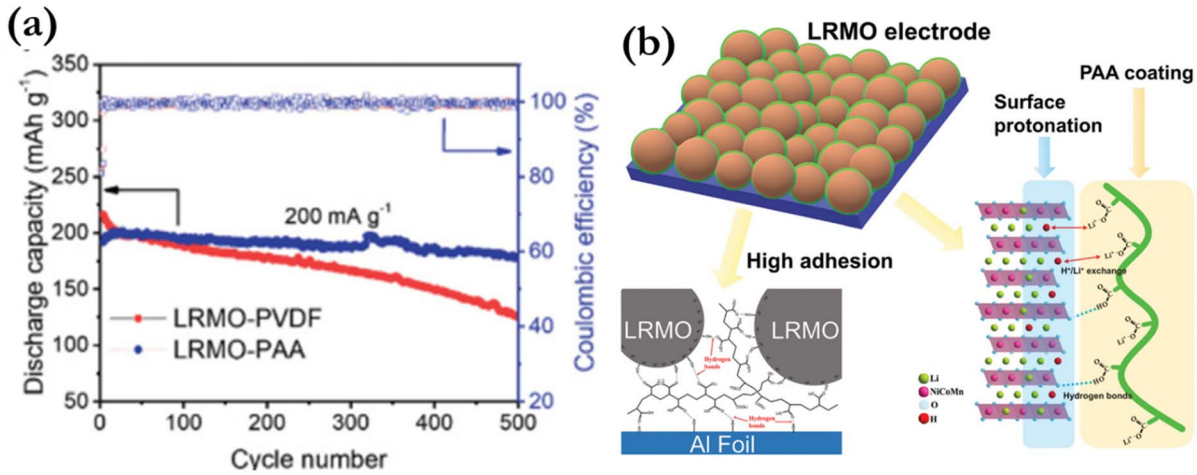

Fig. 12 (a) Cycling performances of the LRMO-PAA and LRMO-PVDF cathodes. (b) Multifunctional protection of the PAA binder for the LRMO cathode. Reproduced with permission from ref. 85. Copyright 2020 WILEY-VCH.

Yang *et al.*[85] demonstrated that a partially protonated PAA binder effectively suppresses voltage fade and capacity degradation in LRMO cathodes. The PAA-modified LRMO exhibited 88% capacity retention over 500 cycles at 200 mA g^{-1} (Fig. 12a) and a reduced voltage fade of 104 mV after 100 cycles. The improved performance was credited to the synergistic surface modification effect of the PAA binder (Fig. 12b) compared to the PVDF-based counterpart.[85] Table 2 presents a comparative summary of the electrochemical performances of cathodes utilizing PAA-based aqueous binders relative to their PVDF-based counterparts.

4.3 Chitosan (CTS)

Chitosan (CTS) is a naturally occurring carbohydrate-based polymer, made up of 1,4-linked glucosamine units, and obtained from the deacetylation of chitin.[6]

Chitin shares a structural similarity to cellulose, differing in the substitution of hydroxyl groups with acetamide groups.[86] Upon deacetylation, the resulting chitosan becomes soluble in dilute acetic acid due to the protonation of glucosamine units ($R–NH_2$ to $R–NH_3^+$).[87,88] Owing to its amino and hydroxyl functional groups, chitosan serves as an effective aqueous-soluble

Table 2 Comparative electrochemical performance of PAA-based cathodes and their PVDF counterparts[a]

Cathode	Binder	IDC mAh g^{-1}	RC mAh g^{-1}	CR (%)	Ref.
$LiFePO_4$	PAA	134.4	N/A	98.8 (50 cycles)	71
	PVDF	125.6	N/A	94.9 (50 cycles)	71
$LiFePO_4$	PAA	144.9 (0.5 C)	N/A	99.4 (100 cycles at 0.5 C)	72
	PVDF	139.5 (0.5 C)	N/A	94.9 (100 cycles at 0.5 C)	72
$LiFePO_4$	2% PAA/1% PVA	161.6 (0.2 C)	130.1 (5 C)	100 (300 cycles at 5 C)	74
	PVA	143 (0.2 C)	77.1 (5 C)	82 (300 cycles at 5 C)	74
$LiFePO_4$	LPPS/PVA/PAA	170 (1 C)	140 (5 C)	99 (200 cycles at 1 C)	75
	PVDF	142 (1 C)	110 (5 C)	63 (200 cycles at 1 C)	75
$LiFePO_4$	PAA	148.09 (0.1 C)	113.4 (1 C)	97.27 (25 cycles at 0.1 C)	76
	PVDF	154.8 (0.1 C)	49 (1 C)		76
$LiMn_2O_4$	PAA	108.1 (0.1 C)	N/A	94.1 (1000 cycles at 1 C)	77
	PVDF	109.4 (0.1 C)	N/A	71.4 (550 cycles at 1 C)	77
$LiFePO_4$	TS–PAALi	156.18 (0.2 C)	105.76 (5 C)	97.47 (100 cycles at 0.2 C)	78
	PVDF	151.62 (0.2 C)	N/A	92.82 (100 cycles at 0.2 C)	78
$LiMn_{1.5}Ni_{0.5}O_4$	LiPAA	N/A	N/A	90 (80 cycles at 0.1 C)	80
	PVDF	N/A	N/A	50 (80 cycles at 0.1 C)	80
NCM811	PAA–PN	229.9 (0.1 C)	167.9 (6 C)	90.41 (200 cycles at 0.5 C)	81
	PVDF	230.2 (0.1 C)	153.8 (6 C)	55.61 (200 cycles at 0.5 C)	81
$Li_{1.2}Mn_{0.6}Ni_{0.2}O_2$	PAA	221.9 (0.1 C)	105.5 (5 C)	75.5 (200 cycles at 1 C)	82
	PVDF	226.4 (0.1 C)	100 (5 C)	70.4 (200 cycles at 1 C)	82
$Li_{1.15}Ni_{0.17}Co_{0.11}Mn_{0.57}O_2$	LiPAA	254.7 (0.1 C)	N/A	90.77 (200 cycles at 0.1 C)	84
	PVDF	223.6 (0.1 C)	N/A	76.21 (200 cycles at 0.1 C)	84
$Li_{1.2}Ni_{0.13}Co_{0.13}Mn_{0.54}O_2$	PAA	244 (0.1 C)	N/A	88 (500 cycles at 4 C)	85
	PVDF	283 (0.1 C)	N/A	58 (500 cycles at 5 C)	85

[a] IDC-initial discharge capacity; RC-rate capability; CR-capacity retention; N/A-not available; and C-rate and number of cycles are given in parentheses.

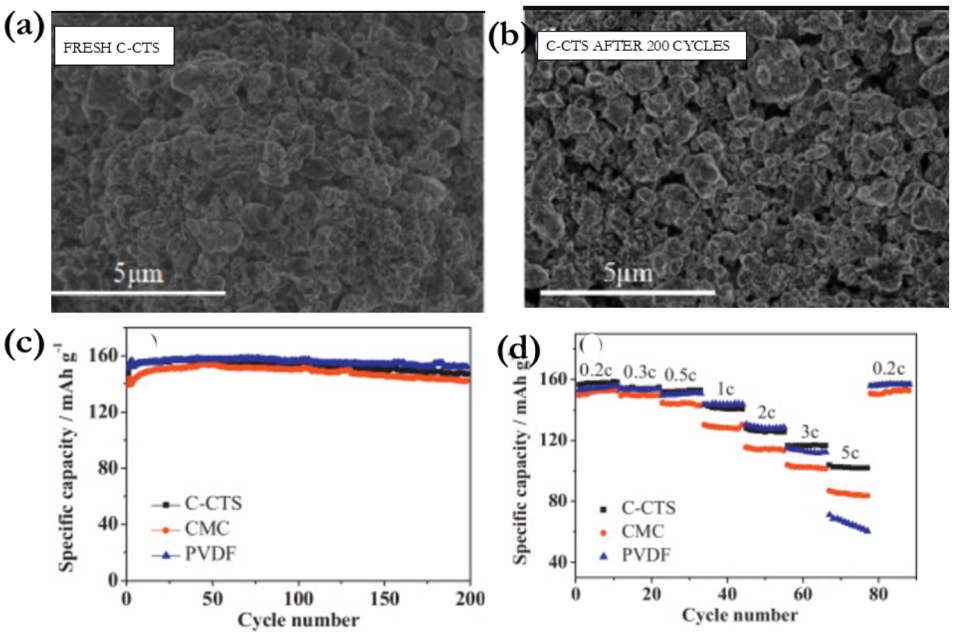

Fig. 13 Morphology of the C-CTS-based $LiFePO_4$ cathode (a) before 200 cycles and (b) after 200 cycles. (c) Cycling performance and (d) rate performance of the $LiFePO_4$ cathode. Reproduced with permission from ref. 89. Copyright 2014, Elsevier.

binder for various cathode materials and can be readily copolymerized or hybridized with functional polymers.[35]

The applicability of chitosan as an aqueous binder for diverse cathode materials is governed by its degree of acetylation (DA) and degree of polymerization (DP), which influence its functional group content and molecular structure. These characteristics enhance its compatibility for copolymerization with other functional polymers.[35,36]

Sun *et al.* first reported the use of carboxymethyl chitosan (C-CTS), an aqueous chitosan derivative, as a binder for $LiFePO_4$ cathodes. The C-CTS-based $LiFePO_4$ retained its structural integrity after 200 cycles, demonstrating its effectiveness (Fig. 13a and b). Although it exhibited slightly lower specific capacity, it outperformed its PVDF counterpart in rate capability and showed comparable cycling stability to PVDF and CMC counterparts (Fig. 13c and d).[89]

Prasanna *et al.*[90] investigated a chitosan-based biopolymer binder for $LiFePO_4$ cathodes in LIBs, comparing its performance to that of conventional PVDF-based cathodes. The chitosan-based electrode exhibited higher ionic conductivity and lower charge transfer resistance, resulting in superior electrochemical performance. Specifically, it gave a capacity of 159.4 mAh g^{-1} with 98.38% capacity retention, compared to 127.9 mAh g^{-1} and 85.13% retention for the PVDF-based counterpart.[90]

Zhong *et al.*[91] employed a C-CTS/PEDOT:PSS composite conductive binder for $LiFePO_4$ cathodes in LIBs. The resulting half-prismatic cell (10 Ah) retained 89.7% capacity at 1 C/2 C over 1000 cycles and exhibited comparable cycling performance to PVDF-based electrodes. Additionally, it showed superior rate capability, maintaining 98% of its 1 C capacity at 7 C, compared to 95.4% for PVDF-based $LiFePO_4$.[91]

He *et al.*[92] enhanced the adhesion strength of carboxymethyl chitosan (C-CTS) by grafting acrylonitrile to introduce cyano groups, forming cyanoethylated C-CTS (CN-CCTS). The CN-CCTS-based $LiFePO_4$ cathode demonstrated superior electrochemical performance, retaining 56.3% of its capacity at 5 C, outperforming its CMC (48.4%) and PVDF (32.8%) counterparts.

Künne *et al.*[93] investigated chitosan binders with varying DP and DA for $LiMn_2O_4$ cathodes in LIBs. Cathodes utilizing low-DP chitosan exhibited twice the adhesion strength of PVDF-based counterparts, enabling reduced binder content and improved specific energy. Chitosan with DA <16% delivered higher capacities than both PVDF and DA >16% formulations. Citric acid cross-linking further enhanced discharge capacity at a 10 C charge rate.[93]

Zhong and coworkers[94] reported that a $LiNi_{0.5}Mn_{1.5}O_4$ cathode employing a carboxymethyl chitosan (C-CTS) binder on carbon-coated aluminum foil exhibited superior electrochemical performance to its PVDF-based counterpart. After 100 cycles, the C-CTS-based electrode retained 95.8% of its capacity, outperforming the PVDF-based electrode (92.9%). At a high rate of 10 C, it delivered a specific capacity of 95.8 mAh g^{-1}, compared to 87.6 mAh g^{-1} for the PVDF-based cathode. The improved performance was attributed to reduced aluminum current collector corrosion, enhanced binder adhesion, and improved lithium-ion diffusion kinetics.[94]

Zhong *et al.*[95] studied the effects of varying mass ratios of a carboxymethyl chitosan/poly(ethylene oxide) (CCTS/PEO) composite binder on the electrochemical performance of 5 V $LiNi_{0.5}Mn_{1.5}O_4$ cathodes. The optimized CCTS/PEO (85 : 15, w/w) binder-based cathode demonstrated superior cycling stability, retaining 81.4% of its initial capacity after 200 cycles at

Table 3 Comparative electrochemical performances of CTS-based cathodes and their PVDF counterparts[a]

Cathode	Binder	IDC mAh g^{-1}	RC mAh g^{-1}	CR (%)	Ref.
$LiFePO_4$	C-CTS	NA	105 (5 C)	N/A	89
	PVDF	NA	105 (5 C)	N/A	89
$LiFePO_4$	CTS	98.30 (1 C)	64.24 (2 C)	90.13 (100 cycles at 0.1 C)	90
	PVDF	68.53 (1 C)	47.83 (2 C)	77.92 (100 cycles at 0.1 C)	90
$LiFePO_4$	CN-CCTS	159.2 (0.2 C)	90 (5 C)	99.2 (100 cycles at 0.2 C)	92
	PVDF	163.4 (0.2 C)	52.2 (5 C)	92.8 (100 cycles at 0.2 C)	92
$LiNi_{0.5}Mn_{1.5}O_4$	CCTS	N/A	95.8 (10 C)	95.8 (100 cycles at 0.2 C)	94
	PVDF	N/A	87.6 (10 C)	92.9 (100 cycles at 0.2 C)	94
$LiNi_{0.5}Mn_{1.5}O_4$	CCTS/PEO	125 (0.2 C)	75 (2 C)	81.4 (200 cycles at 0.5 C)	95
	PVDF	127 (0.2 C)	29 (2 C)	79.8 (200 cycles at 0.5 C)	95
$LiNi_{0.5}Mn_{1.5}O_4$	O-CCTS	121.5 (0.2 C)	95 (3 C)	97.7 (100 cycles at 0.2 C)	97
	O,N-CCTS	112.4 (0.2 C)	85 (3 C)	95.5 (100 cycles at 0.2 C)	97
	PVDF	115.6 (0.2 C)	70 (3 C)	91.6 (100 cycles at 0.2 C)	97

[a] IDC-initial discharge capacity; RC-rate capability; CR-capacity retention; N/A-not available; and C-rate and number of cycles are given in parentheses.

0.5 C, compared to 79.8% for the PVDF-based counterpart. Additionally, the CCTS/PEO-based electrode exhibited enhanced rate capability.[95]

Kuenzel *et al.*[96] evaluated three chitosan grades with varying molecular weights and degrees of deacetylation as aqueous binders for $LiNi_{0.5}Mn_{1.5}O_4$ cathodes. With the incorporation of low molecular weight chitosan (Chi-85 and Chi-99), $LiNi_{0.5}Mn_{1.5}O_4$ exhibited inferior capacity and cycling stability due to inadequate electrode densification and mechanical strength. In contrast, high molecular weight chitosan (Chi-77) enabled improved electrochemical performance. Additionally, citric acid (CA) cross-linking enhanced both rate capability and cycling stability. Co-cross-linking with guar gum further enhanced mechanical integrity and flexibility, enabling high mass loading electrodes with stable specific capacities exceeding 131 mAh g^{-1} at C/3 and 123 mAh g^{-1} at 1 C.[96]

Yu *et al.*[97] studied the electrochemical performance of the $LiNi_{0.5}Mn_{1.5}O_4$ cathode using C-CTS binders with different DS (O-CCTS and O,N-CCTS). The O-CCTS-based LNMO exhibited the highest initial discharge capacity of 123.2 mAh g^{-1}, followed by PVDF (115.7 mAh g^{-1}) and O,N-CCTS (112.9 mAh g^{-1}). After 100 cycles at 0.2 C, O-CCTS retained 97.7% of its capacity, O,N-CCTS retained 95.5%, and PVDF retained 91.6%. Despite its slightly lower capacity, O,N-CCTS-based $LiNi_{0.5}Mn_{1.5}O_4$ demonstrated improved electrochemical performance, likely due to abundant hydrogen bonding facilitating lower impedance and enhanced interfacial stability.[97]

It is noteworthy that although numerous aqueous-based binders have been explored for lithium-ion battery cathode materials, binders such as polytetrafluoroethylene (PTFE), polyvinyl alcohol (PVA), guar gum, xanthan gum, and carrageenan were not discussed in this study due to their limited application in cathode systems. Instead, this work focuses exclusively on the application of CMC, PAA, and CTS-based aqueous binders, which exhibit significant potential for the commercial implementation of lithium-ion battery cathodes. Table 3 presents a comparative summary of the electrochemical performance of cathodes utilizing CTS-based aqueous binders relative to their PVDF-based counterparts.

It is noteworthy that the electrochemical performance of an aqueous-based cathode is largely influenced by the functional groups present in the aqueous binders. Functional groups such as hydroxyl, amine, and carboxyl in CMC, CTS, and PAA play a critical role in modulating electrode–binder interactions, including TM ion coordination and hydrogen bonding at the cathode surface. These interactions promote robust particle cohesion, strong interfacial adhesion, mechanical flexibility, and improved ionic conductivity, thereby maintaining structural integrity during electrochemical cycling. Consequently, they facilitate efficient Li^+ transport, enhance electrode stability, reduce polarization, and improve both capacity retention and coulombic efficiency.

4.4 Other aqueous binders

Sodium alginate (SA), a biopolymer extracted from brown algae, exhibits strong adhesive properties due to its rich carboxylic groups and polymer backbone, which enhance contact with active materials and improve adhesion strength. Also, the coordination of metal cations into an "egg-box" structure enables the chelation of TM ions, thereby mitigating their dissolution from the active material into the electrolyte.[36,98] Bigoni *et al.*[99] utilized SA as a binder for $LiNi_{0.5}Mn_{1.5}O_4$ cathodes and it exhibited superior performance, delivering a specific capacity of 150 mAh g^{-1}, compared to 110 mAh g^{-1} for its PVDF-based counterpart at 2 C. Long-term cycling studies revealed that the alginate-based cathode retained approximately 86% of its initial capacity after 200 cycles, while the PVDF-based counterpart maintained 89% after only 85 cycles. Electrochemical Impedance Spectroscopy (EIS) further confirmed significantly lower charge transfer resistance in the SA binder-based cathode, indicating enhanced interfacial charge transport.[99] Guar gum (GG) and xanthan gum (XG) are aqueous-soluble polysaccharides that are widely used in the food industry, and have attracted attention as potential binders for LIB electrodes. Their highly branched structures, rich in polar functional groups, confer advantageous properties such as rheological properties, mechanical robustness, effective coordination with TM ions, and ease of Li^+ transport within the

electrode matrix.[36,98] Carvalho and coworkers[100] employed GG as a binder in $LiNi_{0.33}Mn_{0.33}Co_{0.33}O_2$ cathodes, which demonstrated excellent electrochemical performance, delivering a specific capacity of 100 mAh g^{-1} at a high rate of 5 C and retaining 85% of its initial capacity after 200 cycles.[100] He and coworkers[101] reported that the XG binder-based $LiFePO_4$ cathode exhibited a stable cycling profile, retaining 96.9% of its initial capacity after 100 cycles.[101]

Overall, it is important to highlight the sustainability aspect of the reported CMC, PAA, CTS, SA, XG, and GG aqueous binders compared to the conventional PVDF binders used in LIB cathode materials. These binders are derived from renewable and bio-based sources, thereby reducing dependence on petroleum-based feedstocks and promoting a circular economy. Moreover, the use of aqueous binders eliminates toxic organic solvents, mitigating greenhouse gas emissions and hazardous waste disposal concerns. Their energy-efficient processing further lowers the overall production cost of LIB cathodes. The adoption of aqueous binders would enhance the safety, sustainability, and circularity of LIB cathode manufacturing while aligning with Sustainable Development Goal 7 (Affordable and Clean Energy).

5 Challenges of aqueous binders

Despite the significant potential of aqueous binder-based electrodes in LIB cathode fabrication, their electrochemical performance is still hindered by challenges such as crack formation, current collector corrosion, and lithium-ion leaching.[6]

The primary challenge associated with the aqueous processing method is the low colloidal stability of the electrode slurry, which significantly hampers the subsequent coating process. This instability arises from strong electrostatic interactions and hydrogen bonding between water molecules and the cathode components. During drying, particularly in thick cathodes required for high energy density applications, these effects promote crack formation within the electrode structure.[6]

The primary limitation of the aqueous-based processing approach lies in the reduced colloidal stability of the electrode slurry, which poses significant challenges during the coating process. This instability is primarily attributed to strong electrostatic interactions and hydrogen bonding between water molecules and the electrode constituents. Consequently, when such colloidal dispersions are employed, crack formation during the drying stage becomes prominent, especially in thick electrodes, which are essential for achieving high energy density.[6,102]

To meet the required high energy density demands of LIBs, thick cathodes (100–200 μm) are typically required. The drying pressure of wet-coated cathodes increases with both coating thickness and mass loading. Notably, an aqueous-processed NMC cathode with an areal loading of ~12.5 mg cm^{-2} remains crack-free. However, slight microcracks begin to appear at ~15 mg cm^{-2}, and further increases in mass loading lead to crack propagation and eventual delamination from the foil because of its reduced interfacial adhesion.[6,103]

Rollag *et al.* investigated the influence of drying temperature and electrode thickness on crack formation in NMC cathodes using SBR binder. Cathodes with areal loadings of 11, 15, and 23 mg cm^{-2} were dried at 20, 45, and 70 °C. Increased drying temperatures (45 and 70 °C) led to the formation of more pores and microcracks due to rapid solvent evaporation and capillary stress. These effects are attributed to enhanced particle sedimentation and limited diffusion during the drying process, particularly in thick electrodes, highlighting the critical role of drying temperature in crack formation.[6,103]

Furthermore, the reaction of metal oxide-based cathode materials with water in LIBs significantly increases the pH of the aqueous slurry due to the formation of hydroxide species. This alkalinity promotes corrosion of the aluminum foil, which typically derives its corrosion resistance from a native aluminum oxide layer (~2 nm thick). This protective layer is robust, self-healing, and stable within a pH range of 4.5–8.5. At higher pH levels, however, the oxide layer undergoes dissolution *via* specific chemical pathways, thereby exposing the underlying aluminum to corrosive attack and impairing its self-passivating capability.[6,104]

The corrosion of the aluminum foil can lead to significant issues, including the generation of hydrogen gas, which becomes trapped within the cathode coating, causing void formation, cracking, and reduced adhesion to the current collector.[105] Additionally, aqueous corrosion products formed at high pH may contaminate the electrolyte and react with the cathode's active material, increasing interfacial resistance. To mitigate these effects, two primary strategies have been employed, one of which involves introducing a weak acid into the slurry prior to coating to lower the pH.[6] To mitigate slurry-induced aluminum corrosion, researchers have traditionally employed two approaches. The first involves the use of weak acids, such as phosphoric acid and formic acid, to reduce the pH of the aqueous slurry.[63,106] The second strategy entails applying a carbon coating (CC) to the aluminum foil to prevent direct contact with the corrosive slurry. For instance, Doberdo *et al.* introduced a carbon interlayer between the active material and the aluminum current collector, which effectively improved interfacial stability, reduced charge transfer resistance, and enhanced the overall cathode performance.[49]

Lithium-ion leaching is also a critical issue arising from the interaction between water and cathode active materials, leading to reduced accessible capacity and the loss of cyclable lithium. Recent studies have demonstrated that phosphoric acid can mitigate these effects in NMC-based cathodes. PA promotes the formation of a protective metal phosphate layer on the NMC particle surface, thereby stabilizing the electrode–electrolyte interface and suppressing lithium and TM dissolution.[6,63]

6 The industrial perspective of aqueous binders

The increasing demand for LIBs in applications such as grid storage, electric vehicles, and portable electronics is driving rapid growth in the binder market. From an industrial

perspective, the cost contribution of binders in various battery chemistries is a critical factor in evaluating economic feasibility. Notably, the choice of binder significantly influences the overall cost structure of battery technologies. The cathode binders contribute approximately 1.4–1.65% of the total cost in ternary cathode LIBs and 2.2–2.5% in $LiFePO_4$ batteries. For instance, the production of a single GWh $LiFePO_4$-based battery typically consumes 2200–2500 tons of cathode material and requires approximately 33–37 tons of imported PVDF binder in China, amounting to a cost of $2.26–2.58 million. Thus, battery commercialization depends heavily on their cost-effectiveness, performance, and safety. These factors are crucial for guiding manufacturers, investors, and researchers in selecting and developing viable battery systems.[107]

Interestingly, aqueous binders offer a promising solution to meet the increasing demand for sustainable energy storage systems. Given concerns over the potential reproductive toxicity of PVDF, aqueous binders are emerging as viable alternatives due to their lower environmental impact and cost. Consequently, battery and materials manufacturers are actively developing cost-effective and eco-friendly aqueous binders with comparable performance to PVDF. Notably, PAA is significantly more affordable than PVDF in single GWh-scale battery production, promoting its adoption. Aqueous binders are therefore particularly well-suited for $LiFePO_4$-based batteries and large-scale energy storage applications.[107]

Furthermore, the advancement of aqueous cathode binder technologies is poised to significantly influence the energy storage industry. Projections estimate that the market value of next-generation aqueous binder technologies could reach approximately $50 million by 2025. Based on recent developments, the production volume of aqueous binders is expected to range from 1500 to 14 500 tons between 2023 and 2025, corresponding to a market value between $57.29 million and $438 million. Moreover, the demand for Chinese-sourced binder materials such as CMC and SBR is anticipated to exceed $400 million, highlighting the substantial commercial potential of aqueous binder systems.[107]

It is important to emphasize that, at present, Chinese companies such as Sumitomo Seika Chemicals Co., Ltd, Shandong Gelon LIB Co., Ltd, and Zeon Corporation are among the major suppliers of commercial aqueous binders for cathode materials. However, the large-scale commercial adoption of aqueous-based binders for LIB cathodes remains in its early stages. To the best of our knowledge, the utilization of aqueous binders by commercial cell manufacturers is still limited.

7 Conclusion and outlook

The rapid expansion of the LIB market, driven by increasing demand for energy storage in consumer electronics and electric vehicles, has intensified research on LIBs. Binders are among the critical components influencing LIB electrochemical performance. Consequently, the development of high-performance binders for both cathodes and anodes has garnered significant attention. While aqueous binders have been widely explored for anode fabrication, their application in cathodes remains challenged by several material-specific issues. Nevertheless, the adoption of aqueous binders for cathode processing represents a significant step toward cost-effective and environmentally sustainable LIB manufacturing.[6,98]

This review comprehensively summarizes recent advancements in the application of aqueous binders for cathode materials in LIBs, with a particular focus on their overview, practical applications (particularly CMC, PAA and CTS binders) and the industrial perspective. Traditionally, cathode fabrication employs PVDF as the binder in conjunction with NMP as the organic solvent to ensure mechanical and electrochemical stability. However, the high cost of fluorinated PVDF and the toxic, teratogenic nature of NMP, which requires complex and costly solvent recovery systems, have prompted increasing interest in environmentally benign, cost-effective aqueous alternatives.

Thus, the exploration of aqueous binders has provided valuable insights into improving the sustainability of LIB cathode manufacturing. $LiFePO_4$ is regarded as the most suitable cathode material for aqueous processing due to its relatively low reactivity with water compared to other conventional cathodes. The superior performance of aqueous binder-based $LiFePO_4$ electrodes is attributed to their well-maintained microstructure, enhanced lithium intercalation/deintercalation kinetics, and reduced swelling of the binder in organic electrolytes. However, the fabrication of high-capacity, high-voltage cathode materials using aqueous binders remains challenging due to their increased sensitivity to moisture.

Water adversely affects the performance of high-voltage cathode materials by promoting lithium leaching *via* cation exchange (Li^+/H^+), leading to elevated slurry pH and the subsequent corrosion of the aluminum current collector. This corrosion induces hydrogen gas evolution and bubble formation within the slurry, ultimately causing electrode cracking during drying. The resulting surface fissures reduce interparticle cohesion, compromising the electrode's structural integrity and electrical connectivity.

To mitigate cracking and lithium ion leaching during the fabrication of high-voltage cathode materials such as NMC, spinel and LRLO, several challenges must be overcome. Binders enriched with carboxylic acid functional groups have demonstrated superior electrochemical performance in Li-rich cathodes. This highlights the potential of exploring naturally derived polymers with high carboxyl group content as promising binder candidates for such cathode systems.

The mitigation of aluminum corrosion during aqueous processing includes pH adjustment of the slurry using mild acids (*e.g.*, phosphoric acid), or applying a carbon coating (CC) to the aluminum foil. The latter also facilitates the formation of a lithium phosphate layer on cathode particles, suppressing TM dissolution. Still, the impacts of trace acid additives on lithium leaching in NMC and LRMO materials remain inconclusive and warrant further investigation. Therefore, in the optimization of the slurry pH, the interactions between acid additives and specific cathode chemistries must be considered since the

optimal additive concentration is closely linked to the structural properties of the active material.

From a commercial perspective, reducing the binder content to ≤3 wt% without compromising mechanical integrity and adhesion is critical for scalable production. Future research should prioritize the industrial-scale implementation of aqueous processing methods for cathode materials. The successful transition from the laboratory to the large-scale manufacturing of water-soluble binder-based LIBs hinges on overcoming challenges such as slurry stability over time and ensuring consistent reproducibility across production batches. In addition, aqueous binders should be developed for next-generation solid-state and Li–S battery cathode materials. Aqueous binders obtained from bio-derived polymers are another area of interest in the future application of these materials in LIBs. Aqueous processing of cathode materials presents promising opportunities to revolutionize cathode fabrication, contributing significantly to the sustainability and efficiency of LIB technologies.

Author contributions

Samuel O. Ajayi: conceptualization and writing – original draft; Tarekegn H. Dolla: writing – original draft; and Peter R. Makgwane, Xinying Liu, Moses M. Solomon, Cyril O. Ehi-Eromosele, Mkhulu K. Mathe: writing – review & editing, supervision.

Conflicts of interest

The authors declare no conflicts of interest.

Data availability

No data were used for the research described in the article.

Acknowledgements

The authors are grateful to the University of South Africa (UNISA) for the financial support provided.

References

1 J. Li, Z. Wu, Y. Lu, Y. Zhou, Q. Huang, L. Huang and S. Sun, *Adv. Energy Mater.*, 2017, **7**, 1701185.
2 M. Armand and J. Tarascon, *Buiding Better Batteries*, 2008, **451**, 2–7.
3 A. Fotouhi, D. J. Auger, K. Propp, S. Longo and M. Wild, *Renew. Sustain. Energy Rev.*, 2016, **56**, 1008–1021.
4 G.-L. Xu, Q. Wang, J.-C. Fang, Y.-F. Xu, J.-T. Li, L. Huang and S.-G. Sun, *J. Mater. Chem. A*, 2014, **2**, 19941–19962.
5 S.-L. Chou, Y. Pan, J.-Z. Wang, H.-K. Liu and S.-X. Dou, *Phys. Chem. Chem. Phys.*, 2014, **16**, 20347–20359.
6 A. M. Pillai, P. S. Salini, B. John and M. T. Devassy, *Energy Fuels*, 2022, **36**, 5063–5087.
7 P. S. Salini, S. V Gopinadh, A. Kalpakasseri, B. John and M. Thelakkattu Devassy, *ACS Sustain. Chem. Eng.*, 2020, **8**, 4003–4025.
8 A. Chakraborty, S. Kunnikuruvan, S. Kumar, B. Markovsky, D. Aurbach, M. Dixit and D. T. Major, *Chem. Mater.*, 2020, **32**, 915–952.
9 A. Manthiram, *Nat. Commun.*, 2020, **11**, 1550.
10 F. Wu, J. Maier and Y. Yu, *Chem. Soc. Rev.*, 2020, **49**, 1569–1614.
11 B. John and G. Cheruvally, *Polym. Adv. Technol.*, 2017, **28**, 1528–1538.
12 S. Zhang, J. Ma, Z. Hu, G. Cui and L. Chen, *Chem. Mater.*, 2019, **31**, 6033–6065.
13 R. Jung, M. Metzger, F. Maglia, C. Stinner and H. A. Gasteiger, *J. Electrochem. Soc.*, 2017, **164**, A1361–A1377.
14 D. Wang, W. Liu, X. Zhang, Y. Huang, M. Xu and W. Xiao, *Int. J. Photoenergy*, 2019, **2019**, 2730849.
15 R. Jung, M. Metzger, F. Maglia, C. Stinner and H. A. Gasteiger, *J. Phys. Chem. Lett.*, 2017, **8**, 4820–4825.
16 D. Andre, S.-J. Kim, P. Lamp, S. F. Lux, F. Maglia, O. Paschos and B. Stiaszny, *J. Mater. Chem. A*, 2015, **3**, 6709–6732.
17 M. Zhao, B. Zhang, G. Huang, W. Dai, F. Wang and X. Song, *Energy Fuels*, 2012, **26**, 1214–1219.
18 B. John, C. P. Sandhya and C. Gouri, *Nanomaterials*, 2018, 343–398.
19 P. K. Nayak, E. M. Erickson, F. Schipper, T. R. Penki, N. Munichandraiah, P. Adelhelm, H. Sclar, F. Amalraj, B. Markovsky and D. Aurbach, *Adv. Energy Mater.*, 2018, **8**, 1702397.
20 H. Pan, S. Zhang, J. Chen, M. Gao, Y. Liu, T. Zhu and Y. Jiang, *Mol. Syst. Des. Eng.*, 2018, **3**, 748–803.
21 S.-T. Myung, F. Maglia, K.-J. Park, C. S. Yoon, P. Lamp, S.-J. Kim and Y.-K. Sun, *ACS Energy Lett.*, 2017, **2**, 196–223.
22 Y. Wang, E. Wang, X. Zhang and H. Yu, *Energy Fuels*, 2021, **35**, 1918–1932.
23 M. Zubair, G. Li, B. Wang, L. Wang and H. Yu, *ACS Appl. Energy Mater.*, 2018, **2**, 503–512.
24 R. Lin, E. Hu, M. Liu, Y. Wang, H. Cheng, J. Wu, J.-C. Zheng, Q. Wu, S. Bak and X. Tong, *Nat. Commun.*, 2019, **10**, 1650.
25 H. Hu, M. Zhang, D. Zhang, R. Murakami, P. Wang, Y. Yan and Z. Li, *Mater. Res. Express*, 2019, **6**, 115547.
26 J. Ye, Y. Li, L. Zhang, X. Zhang, M. Han, P. He and H. Zhou, *ACS Appl. Mater. Interfaces*, 2016, **8**, 208–214.
27 S. O. Ajayi, T. H. Dolla, I. T. Bello, X. Liu, P. R. Makgwane, M. K. Mathe and C. O. Ehi-Eromosele, *Inorg. Chem. Commun.*, 2024, 113721.
28 S. O. Ajayi and K. O. Ajanaku, in *IOP Conference Series: Earth and Environmental Science*, IOP Publishing, 2022, vol. 1054, p. 12011.
29 S. O. Ajayi, C. O. Ehi-Eromosele, K. O. Ajanaku and J. A. Adekoya, *J. Mater. Sci. Mater. Electron.*, 2022, **33**, 18716–18725.
30 S. O. Ajayi, C. O. Ehi-Eromosele and K. O. Ajanaku, *Ceram. Int.*, 2022, **48**, 2306–2316.
31 D. Bresser, D. Buchholz, A. Moretti, A. Varzi and S. Passerini, *Energy Environ. Sci.*, 2018, **11**, 3096–3127.
32 S. Feng, Z. Zhong, Y. Wang, W. Xing and E. Drioli, *J. Memb. Sci.*, 2018, **549**, 332–349.

33 T. Tanabe, T. Gunji, Y. Honma, K. Miyamoto, T. Tsuda, Y. Mochizuki, S. Kaneko, S. Ugawa, H. Lee and T. Ohsaka, *Electrochim. Acta*, 2017, **224**, 429–438.
34 K. Notake, T. Gunji, H. Kokubun, S. Kosemura, Y. Mochizuki, T. Tanabe, S. Kaneko, S. Ugawa, H. Lee and F. Matsumoto, *J. Appl. Electrochem.*, 2016, **46**, 267–278.
35 M. Srivastava, A. K. MR and K. Zaghib, *Batteries*, 2024, **10**, 268.
36 N. Lingappan, L. Kong and M. Pecht, *Renew. Sustain. Energy Rev.*, 2021, **147**, 111227.
37 R. Wang, L. Feng, W. Yang, Y. Zhang, Y. Zhang, W. Bai, B. Liu, W. Zhang, Y. Chuan and Z. Zheng, *Nanoscale Res. Lett.*, 2017, **12**, 1–11.
38 A. Guerfi, M. Kaneko, M. Petitclerc, M. Mori and K. Zaghib, *J. Power Sources*, 2007, **163**, 1047–1052.
39 S. F. Lux, F. Schappacher, A. Balducci, S. Passerini and M. Winter, *J. Electrochem. Soc.*, 2010, **157**, A320.
40 S. Yang, Y. Huang, S. Su, G. Han and J. Liu, *Powder Technol.*, 2019, **351**, 203–211.
41 G. T. Kim, S. S. Jeong, M. Joost, E. Rocca, M. Winter, S. Passerini and A. Balducci, *J. Power Sources*, 2011, **196**, 2187–2194.
42 L. Qiu, Z. Shao, D. Wang, F. Wang, W. Wang and J. Wang, *Carbohydr. Polym.*, 2014, **112**, 532–538.
43 S. N. Eliseeva, O. V Levin, E. G. Tolstopjatova, E. V Alekseeva, R. V Apraksin and V. V Kondratiev, *Mater. Lett.*, 2015, **161**, 117–119.
44 W. Zheng, S. Zhou, X. Yang, P. Wang, N. Luo, X. Hu, Y. Cai and L. Qiu, *J. Appl. Electrochem.*, 2025, **1–15**.
45 C.-C. Li and Y.-W. Wang, *J. Power Sources*, 2013, **227**, 204–210.
46 C.-C. Li, J.-T. Lee, Y.-L. Tung and C.-R. Yang, *J. Mater. Sci.*, 2007, **42**, 5773–5777.
47 S. Chen, H. Zhu, J. Li, Z. Yin, T. Chen, X. Yao, W. Zhao, H. Xue, X. Jiang and Y. Li, *Angew. Chem., Int. Ed.*, 2025, **64**, e202423796.
48 J. Xu, S.-L. Chou, Q. Gu, H.-K. Liu and S.-X. Dou, *J. Power Sources*, 2013, **225**, 172–178.
49 I. Doberdò, N. Löffler, N. Laszczynski, D. Cericola, N. Penazzi, S. Bodoardo, G.-T. Kim and S. Passerini, *J. Power Sources*, 2014, **248**, 1000–1006.
50 N. Loeffler, J. von Zamory, N. Laszczynski, I. Doberdo, G.-T. Kim and S. Passerini, *J. Power Sources*, 2014, **248**, 915–922.
51 A. Kukay, R. Sahore, A. Parejiya, W. B. Hawley, J. Li and D. L. Wood III, *J. Colloid Interface Sci.*, 2021, **581**, 635–643.
52 R. Demiryürek, N. Gürbüz, G. Hatipoglu, M. Er, H. Malkoc, O. Guleryuz, G. Uyar, D. Uzun and M. N. Ateş, *Int. J. Energy Res.*, 2021, **45**, 21182–21194.
53 P. Zhu, J. Han and W. Pfleging, *Nanomaterials*, 2021, **11**, 1840.
54 Z. Chen, G.-T. Kim, D. Chao, N. Loeffler, M. Copley, J. Lin, Z. Shen and S. Passerini, *J. Power Sources*, 2017, **372**, 180–187.
55 S. S. Varshni and A. V. Murugan, *Energy Fuels*, 2025.
56 F. De Giorgio, N. Laszczynski, J. von Zamory, M. Mastragostino, C. Arbizzani and S. Passerini, *ChemSusChem*, 2017, **10**, 379–386.
57 G. T. Pace, H. Wang, J. F. Whitacre and W. Wu, *Nano Sel.*, 2021, **2**, 939–947.
58 I. Dienwiebel, M. Diehl, B. Heidrich, X. Yang, M. Winter and M. Börner, *Adv. Energy Sustain. Res.*, 2021, **2**, 2100075.
59 Z. Wang, N. Dupré, A.-C. Gaillot, B. Lestriez, J.-F. Martin, L. Daniel, S. Patoux and D. Guyomard, *Electrochim. Acta*, 2012, **62**, 77–83.
60 J. Li, R. Klöpsch, S. Nowak, M. Kunze, M. Winter and S. Passerini, *J. Power Sources*, 2011, **196**, 7687–7691.
61 T. Zhao, Y. Meng, R. Ji, F. Wu, L. Li and R. Chen, *J. Alloys Compd.*, 2019, **811**, 152060.
62 S. Zhang, H. Gu, H. Pan, S. Yang, W. Du, X. Li, M. Gao, Y. Liu, M. Zhu and L. Ouyang, *Adv. Energy Mater.*, 2017, **7**, 1601066.
63 A. Kazzazi, D. Bresser, A. Birrozzi, J. von Zamory, M. Hekmatfar and S. Passerini, *ACS Appl. Mater. Interfaces*, 2018, **10**, 17214–17222.
64 Z. Ding, Y. Huang, F. Li, R. Li, H. Lin, J. Li, R. Song, K. Luo and Y. Ren, *J. Colloid Interface Sci.*, 2024, **665**, 80–87.
65 M. Su, Y. Yang, K. Jin, L. Li, H. Tian, Z. Wu, S. He, Y. Liu, C. Zheng and J. Gan, *Energy Fuels*, 2025, **39**, 7890–7900.
66 M. Akhilash, P. S. Salini, B. John, S. Sujatha and T. D. Mercy, *RSC Sustain.*, 2024, **2**, 416–424.
67 Z. Zhang, T. Zeng, Y. Lai, M. Jia and J. Li, *J. Power Sources*, 2014, **247**, 1–8.
68 Q. Fan, W. Zhang, J. Duan, K. Hong, L. Xue and Y. Huang, *Electrochim. Acta*, 2015, **174**, 970–977.
69 B. Hu, I. A. Shkrob, S. Zhang, L. Zhang, J. Zhang, Y. Li, C. Liao, Z. Zhang, W. Lu and L. Zhang, *J. Power Sources*, 2018, **378**, 671–676.
70 F. Sun and D. R. Wheeler, *J. Electrochem. Soc.*, 2023, **170**, 80502.
71 Z. P. Cai, Y. Liang, W. S. Li, L. D. Xing and Y. H. Liao, *J. Power Sources*, 2009, **189**, 547–551.
72 Z. Zhang, T. Zeng, H. Lu, M. Jia, J. Li and Y. Lai, *ECS Electrochem. Lett.*, 2012, **1**, A74.
73 J. Chong, S. Xun, H. Zheng, X. Song, G. Liu, P. Ridgway, J. Q. Wang and V. S. Battaglia, *J. Power Sources*, 2011, **196**, 7707–7714.
74 J. Sun, X. Ren, Z. Li, W. Tian, Y. Zheng, L. Wang and G. Liang, *J. Alloys Compd.*, 2019, **783**, 379–386.
75 C.-Y. Wu and J.-G. Duh, *Electrochim. Acta*, 2019, **294**, 22–27.
76 T. T. B. Vo, M. T. Nguyen, T. L. Pham, T. T. Nguyen, V. G. Tran, V. M. Tran and P. M. L. Le, *Energy Storage*, 2024, **6**, e70006.
77 C. Shen, H. Yu, Z. Xue, G. Hu, Y. Cao, Z. Peng and K. Du, *Chem. Eng. J.*, 2024, **489**, 151287.
78 J. He, H. Zhong and L. Zhang, *J. Appl. Polym. Sci.*, 2018, **135**, 46132.
79 A. Mathew, W. van Ekeren, R. Andersson, M. J. Lacey, S. K. Heiskanen, R. Younesi and D. Brandell, *J. Electrochem. Soc.*, 2024, **171**, 20531.

80 N. P. W. Pieczonka, V. Borgel, B. Ziv, N. Leifer, V. Dargel, D. Aurbach, J. Kim, Z. Liu, X. Huang and S. A. Krachkovskiy, *Adv. Energy Mater.*, 2015, **5**, 1501008.
81 H. Wang, F. Zhang, N. Qin, Z. Wang, Y. Wang, Z. Wang, C. Zeng, H. Li, Q. Liu and Y. Li, *ACS Energy Lett.*, 2024, **10**, 136–144.
82 T. Li, Y. Xiao, X. Hao, Y. Li and W. Wang, *Carbon*, 2024, **228**, 119309.
83 T. Zhao, L. Chang, R. Ji, S. Chen, X. Jin, Y. Zheng, X. Huang, J. Shen and Y. Zhang, *J. Mater. Sci. Mater. Electron.*, 2022, **33**, 16383–16395.
84 M. Yu, Y. Wang, Z. Wang, Y. Fan, J. Song, D. Zhou, K. Wang, Q. Zhang, H. Gu and J. Xie, *J. Electrochem. Soc.*, 2019, **166**, A4122.
85 J. Yang, P. Li, F. Zhong, X. Feng, W. Chen, X. Ai, H. Yang, D. Xia and Y. Cao, *Adv. Energy Mater.*, 2020, **10**, 1904264.
86 D. A. Gopakumar, A. R. Pai, D. Pasquini, L. S.-Y. Ben, A. K. HPS and S. Thomas, *Nanoscale Mater. Water Purif.*, 2019, 1–24.
87 S. Cord-Landwehr and B. M. Moerschbacher, *Fungal Biol. Biotechnol.*, 2021, **8**, 19.
88 L. Yue, L. Zhang and H. Zhong, *J. Power Sources*, 2014, **247**, 327–331.
89 M. Sun, H. Zhong, S. Jiao, H. Shao and L. Zhang, *Electrochim. Acta*, 2014, **127**, 239–244.
90 K. Prasanna, T. Subburaj, Y. N. Jo, W. J. Lee and C. W. Lee, *ACS Appl. Mater. Interfaces*, 2015, **7**, 7884–7890.
91 H. Zhong, A. He, J. Lu, M. Sun, J. He and L. Zhang, *J. Power Sources*, 2016, **336**, 107–114.
92 J. He, J. Wang, H. Zhong, J. Ding and L. Zhang, *Electrochim. Acta*, 2015, **182**, 900–907.
93 S. Künne, F. Püttmann, M. Linhorst, B. M. Moerschbacher, M. Winter, J. Li and T. Placke, *ChemElectroChem*, 2022, **9**, e202200600.
94 H. Zhong, J. He and L. Zhang, *Mater. Res. Bull.*, 2017, **93**, 194–200.
95 H. Zhong, J. Lu, A. He, M. Sun, J. He and L. Zhang, *J. Mater. Sci. Technol.*, 2017, **33**, 763–767.
96 M. Kuenzel, R. Porhiel, D. Bresser, J. Asenbauer, P. Axmann, M. Wohlfahrt-Mehrens and S. Passerini, *Batter. Supercaps*, 2020, **3**, 155–164.
97 N. Yu, J. Ke, L. Li and Y. Bi, *Electrochim. Acta*, 2023, **443**, 141903.
98 A. C. Rolandi, I. de Meatza, N. Casado, M. Forsyth, D. Mecerreyes and C. Pozo-Gonzalo, *RSC Sustain.*, 2024, **2**, 2125–2149.
99 F. Bigoni, F. De Giorgio, F. Soavi and C. Arbizzani, *J. Electrochem. Soc.*, 2016, **164**, A6171.
100 D. V. Carvalho, N. Loeffler, M. Hekmatfar, A. Moretti, G.-T. Kim and S. Passerini, *Electrochim. Acta*, 2018, **265**, 89–97.
101 J. He, H. Zhong, J. Wang and L. Zhang, *J. Alloys Compd.*, 2017, **714**, 409–418.
102 K. B. Singh and M. S. Tirumkudulu, *Phys. Rev. Lett.*, 2007, **98**, 218302.
103 K. Rollag, D. Juarez-Robles, Z. Du, D. L. Wood III and P. P. Mukherjee, *ACS Appl. Energy Mater.*, 2019, **2**, 4464–4476.
104 W. Bauer, F. A. Çetinel, M. Müller and U. Kaufmann, *Electrochim. Acta*, 2019, **317**, 112–119.
105 R. Sahore, D. L. Wood III, A. Kukay, K. M. Grady, J. Li and I. Belharouak, *ACS Sustain. Chem. Eng.*, 2020, **8**, 3162–3169.
106 N. Loeffler, G. Kim, F. Mueller, T. Diemant, J. Kim, R. J. Behm and S. Passerini, *ChemSusChem*, 2016, **9**, 1112–1117.
107 C. Su, X. Gao, K. Liu, Y. Dai, H. Dong, Y. Liu, J. Zhu, Q. Zhang, H. He and G. He, *Nano Res. Energy*, 2024, **3**, e9120094.